INVESTIGATING THE EFFECT OF C-TERMINAL TRUNCATED APOLIPOPROTEIN E4 ON AMYLOID-BETA-INDUCED NEURONAL AND BEHAVIORAL DEFICITS IN MICE

by

Nga Bien-Ly

DISSERTATION

Submitted in partial satisfaction of the requirements for the degree of

DOCTOR OF PHILOSOPHY

in

BIOMEDICAL SCIENCES

in the

GRADUATE DIVISION

of the

UNIVERSITY OF CALIFORNIA, SAN FRANCISCO

I dedicate this dissertation to my parents.

ACKNOWLEDGEMENTS

I'd like to first acknowledge the assistance and guidance of my committee members, Dr. Steven Finkbeiner, Dr. Raymond Swanson, and Dr. Yadong Huang. Their valuable time and effort spent on reading my manuscript drafts and in troubleshooting my projects during committee meetings was deeply appreciated. In particular I'd like to acknowledge the guidance of Yadong who unselfishly donated countless hours over the past five years in helping me further grow and mature as a scientist. In addition to his direct role in mentoring, he is responsible for surrounding me with a great supporting environment embodied by our lab members and our resources and equipment.

Beyond my direct faculty mentors, many other past and present colleagues need to be acknowledged for their contributions towards my overall achievements thus far. There are three individuals from Gladstone that are directly responsible for encouraging me to apply for graduate school at UCSF: Dr. Jeannie Chin, Dr. Kimberly Scearce-Levie, and especially Dr. Jorge Palop, for which I will be forever grateful. The time I spent working with them in the lab of Dr. Lennart Mucke, for whom I am also thankful for that uniquely rewarding opportunity, made me realize how enjoyable pursuing science could be. I also thank Dr. Robert Mahley and Dr. Karl Weisgraber who have kindly shared their wealth of apoE knowledge and reagents that contributed to my thesis and research. I'd also like to acknowledge the tremendous help I received from Dr. Gary Howard and Stephen Ordway for their editorial advice over the years on abstracts and manuscripts.

The entire Huang lab deserves my heartfelt thanks for all of the precious help and support that they've given me these past few years, in particular Walter Brecht, Dennis Miranda, Victoria Yoon, Mary Jeong, and David Walker. I thank Qin Xu and Reeny

Balestra for kindly welcoming me into the lab with open arms and showing me the ropes. Aubrey Bernardo provided not only her excellent technical help but also offered her invaluable friendship to me for which I am forever thankful for. I thank Yaisa Andrews-Zwilling for our fruitful collaborations, and along with Karen Ring for their friendship, and in making the lab a fun and lively environment. I thank Yadong again for giving me the precious opportunity to mentor Charles Wang and for his contributions to my research.

I wouldn't have been able to accomplish anything though, if not for my family. Their continued love and support has kept me inspired to keep pursuing my education and keep striving for better. My dad's motto, "Never stop," is something I hold near and dear and will keep me motivated onwards to the next step in my career. I also want to thank my surrogate and future in-law family for enduring graduate school with me and taking me in as one of their own.

Last, but certainly not least, I want to thank my fiancé Wilbert Mui for his unwavering love, support, advice, friendship, and sense of humor, all of which contributed to making graduate school not only bearable but absolutely enjoyable.

CONTRIBUTIONS

Parts of the text and figures of this dissertation are a reprint of the material as it appears in Bien-Ly N *et al.* (*PNAS,* 2011, 108(10):4236-4241), which was published on 8 March 2011. Specifically, the Results shown in Chapter 3, the Discussion of Chapter 4, and the Materials and Methods contained in Chapter 2 have largely appeared in that publication. The contents of Chapter 1 (Introduction and Literature Review) are unpublished material as is Chapter 5, the proposed Future Studies.

The specific contributions by the coauthors were of a supportive and collaborative nature and the findings described in this work are equivalent to that of a standard thesis or dissertation by an individual PhD candidate. Yaisa Andrews-Zwilling collaborated by performing the mouse behavioral studies. Qin Xu contributed to the project by starting the original mouse breeding. Aubrey Bernardo provided technical support and Charles Wang was a student intern that assisted with data collection. Yadong Huang was the principle investigator, supervised the project, and assisted with the writing of the published manuscript.

ABSTRACT

Investigating the Effect of C-Terminal Truncated Apolipoprotein E4 on Amyloid-beta-Induced Neuronal and Behavioral Deficits in Transgenic Mice

Nga Bien-Ly

Among the common apolipoprotein (apo) E isoforms (apoE2, apoE3, and apoE4), apoE4 is the major known genetic risk factor for Alzheimer's disease (AD). Previous *in vitro* and *in vivo* experiments showed that apoE4 preferentially undergoes aberrant cleavage in neurons, yielding neurotoxic C-terminal-truncated fragments. To study the effect of these fragments on amyloid-β (Aβ) clearance/deposition and their potential synergy with Aβ in eliciting neuronal and behavioral deficits, transgenic mice expressing human apoE3, apoE4, or apoE4(Δ272–299) were cross-bred with mice expressing human amyloid precursor protein (hAPP) harboring familial AD mutations ($hAPP_{FAD}$). At 6–8 months of age, $hAPP_{FAD}$ mice expressing human apoE3 or apoE4 had 94% and 89% less hippocampal $Aβ_{1-x}$, respectively, than hAPP mice lacking apoE, while $hAPP_{FAD}$ mice expressing mouse apoE had the highest Aβ levels. Aβ deposition in $hAPP_{FAD}$ mice expressing human apoE3 or apoE4 was 89% and 87% less than $hAPP_{FAD}$ mice without apoE, respectively. Thus, human apoE stimulates Aβ clearance, but mouse apoE does not. Expression of apoE4(Δ272–299) reduced total Aβ levels by only 63% and Aβ deposition by 46%, compared to $hAPP_{FAD}$ mice without apoE. Unlike apoE3 and apoE4, the C-terminal-truncated apoE4 bound Aβ peptides poorly, leading to decreased Aβ clearance and increased Aβ deposition. Despite their lower levels of Aβ and Aβ

deposition, $hAPP_{FAD}$/apoE4(Δ272–299) mice accumulated potential pathogenic Aβ oligomers and displayed neuronal and behavioral deficits similar to or more severe than those in $hAPP_{FAD}$ mice lacking apoE. Thus, the C-terminal-truncated apoE4 fragment inefficiently clears Aβ peptides and has enhanced toxicity in the presence of low levels of Aβ to elicit neuronal and behavioral deficits in mice.

TABLE OF CONTENTS

LIST OF FIGURES

CHAPTER 1

Introduction / Literature Review

Alzheimer's Disease and the Amyloid-Cascade Hypothesis

AD is one of the primary causes of dementia in the elderly and currently afflicts more than 5 million people in the United States and 15 million worldwide. Within the next 20 years, these numbers are projected to double (1). Despite intensive ongoing research efforts, the causes of sporadic AD or an effective treatment have not yet been identified. Sporadic, late-onset AD (symptoms after the age of 60) occurs in more than 95% of all cases and has unknown causes. The less common, early-onset forms of AD (symptoms before the age of 60) that occur in less than 5% of affected populations are linked to autosomal dominant mutations in the amyloid precursor protein (APP) gene or its processing enzymes presinilin-1 and -2 (PS1, PS2) (2). These mutations alter the production of the neurotoxic Aβ peptides which may contribute to early AD onset (2).

The normal cleavage of APP, a transmembrane protein highly expressed in neurons, yields larger N-terminal products (APPsα or APPsβ) or Aβ, depending on the sequence of proteolysis (3). The physiological function of APP is still unclear, however there is recent evidence for its requirement at neuromuscular junctions to mediate synaptic transmission and plasticity (4). Likewise, the physiological role of Aβ has not yet been fully understood. Limited studies have suggested that Aβ is released from APP in response to synaptic activity in hippocampal slices and *in vivo* into interstitial fluid and may enhance neural plasticity and memory (3, 5, 6). How exactly Aβ functions at the

synapse though, either to mediate selective depression through interaction with receptors or as a general feedback in response to increases in activity, and its dysregulation in AD pathogenesis remain critical questions (3).

Disruptions in Aβ homeostasis have been implicated in the global cognitive decline and progressive neurodegeneration in AD patients (7). As a result, the 4.5-kDa Aβ peptide (containing 39–43 amino acid residues), the central component of the amyloid hypothesis, is a major focus of AD research. The genetic evidence supporting the amyloid hypothesis comes from families with inherited mutations in APP, PS1, or PS2 that have altered Aβ production and develop early dementia. Overwhelming accumulation of Aβ and a possible lack of effective clearance lead to the extracellular deposition of amyloid as plaques, originally hypothesized to induce gradual synapse loss, neurofibrillary tangles of hyperphosphorylated tau, and neuronal death. Amyloid plaques are more frequently composed of $A\beta_{42}$ than $A\beta_{40}$ because it more readily forms β-sheets and β-fibrils in an energetically favored process (8, 9). These fibrillar species of Aβ were assumed to initiate primary pathologies by depositing into plaques and ultimately compromising the integrity of neurons.

Recent insights into Aβ pathological mechanisms have focused on the neurotoxic effects of oligomeric forms of Aβ, originally identified and isolated from APP expressing cell lines (10, 11). These pre-fibrillar Aβ assemblies gained more interest with emerging evidence that Aβ-induced synaptic loss begins before the onset of amyloid deposition (12), and that plaques do not correlate well with neuropathology in AD transgenic mouse models (13-16). In fact, the J20 line of transgenic mice expressing human APP harboring familial AD mutations ($hAPP_{FAD}$) accumulates neurotoxic Aβ peptides and displays

synaptic and cognitive deficits at 5–6 months of age without obvious plaque pathology (12, 14, 15). In the TG2576 transgenic mice expressing $hAPP_{FAD}$ with the Swedish mutations under a prion promoter, a 12-mer of Aβ termed Aβ*56 was identified as the principle culprit behind functional and behavioral deficits; Aβ*56 is also found in human AD brain samples (17). In addition, smaller Aβ aggregates of 17–22 kDa, termed Aβ-derived diffusible ligands (ADDLs), blocked LTP and induced neuronal death in slice-culture systems (18). Aβ dimers and trimers have also been implicated as the neurotoxic species *in vivo* in recent studies (19-21).

Neurobiology of ApoE

ApoE, a component of many lipoproteins involved in systemic lipid transport, is expressed in different tissues and cell types throughout the body (22). In addition to its actions in the periphery, apoE plays a significant role within the central nervous system (CNS) as the major resident apolipoprotein for cholesterol redistribution (22-25).

Human apoE exists in three isoforms, each containing 299 amino acids with a molecular mass of 34.2 kDa. The differences between isoforms occur at residues 112 and 158: apoE2 has a cysteine at both sites, apoE3 has cysteine-112 and arginine-158, and apoE4 has arginines at both sites (22). The frequency of occurrence for the apoE alleles are 5–10% for apoE ε2, 70–80% for apoE ε3, and 10–15% for apoE ε4 (22). Structurally, these single amino acid changes result in dramatic conformational and functional differences. ApoE2 is associated with recessive type III hyperlipoproteinemia, due to defective receptor binding caused by the presence of cysteine-158 (22, 26). Likewise, arginine-112 in apoE4 results in domain interaction between the N- and C-termini of

apoE and decreases its overall protein stability (26, 27). Consequently, apoE4 is more prone to unfolding into a molten globular state than apoE3 or apoE2 (27). The apoE4 isoform is more susceptible to aberrant proteolytic cleavage, yielding toxic fragments that may impair normal neuronal function (24, 28-30). The lipid binding domain of apoE4 is less organized, and C-terminal truncation weakens the lipoprotein binding ability of both isoforms (31). Importantly, the lipid-binding domain of apoE is necessary and sufficient for lipid efflux from cells and for the assembly of apoE-containing nascent high-density lipoprotein particles (pre-β-HDL) mediated by ABCA1, an intracellular lipid transporter (32).

In the CNS, apoE is synthesized mainly by astrocytes and activated microglia, and its mRNA levels in the brain are second highest to the liver (33, 34). The proposed function of apoE secreted by astrocytes is to aid in neurite extension and synaptogenesis (35), whereas neurons produce apoE under stress or injury, when additional lipid exchange for repairs and remodeling is required (24, 36, 37). Functional differences between the isoforms include the stimulation of neurite outgrowth and synaptogenesis by apoE3 and inhibition of these critical processes by apoE4 (38-41). ApoE4 is associated with poor clinical outcome after traumatic brain injury or ischemic stress to the CNS, while local expression of apoE3 is stimulated at acute hippocampal lesions (42-44). Also, isoform-dependent differences in LTP magnitude were observed in slice cultures from mice expressing the human apoE gene knocked into the mouse apoE locus and controlled by the endogenous mouse promoter (apoE3 = WT > apoE-/- and apoE4) (45).

ApoE Polymorphisms and Alzheimer's Disease

Aβ plaques and neurofibrillary tangles (NFTs) are the classical pathological hallmarks of AD. Early studies characterizing the proteins contained within Aβ deposits and NFTs identified apoE as a constituent of both (46-48). Levels of parenchymal Aβ deposition and the apoE4 genotype correlate strongly in AD patients (49). Since then, apoE4 has been identified as the major genetic risk factor for AD; it increases the occurrence and lowers the age of onset of AD as compared to apoE3 (50-52). On the other hand, apoE2 carriers in certain populations have a lower risk of developing AD as compared to apoE3/3 homozygotes (53).

How apoE4 specifically contributes either directly or indirectly to the development of Alzheimer's disease is unclear. Several mouse models have been established to study the direct roles of apoE4 in AD pathogenesis. Neuron-specific apoE4 transgenic mice (NSE-apoE4) develop neuronal and spatial learning and memory deficits (54-56). Astrocyte-specific apoE4 transgenic mice (GFAP-apoE4) display working memory deficits without significant neuronal deficits (57). ApoE4 knock-in (apoE4-KI) mice also develop neuronal and behavioral deficits (58, 59).

There are many hypotheses regarding apoE4's mechanistic roles in AD pathogenesis, and they can be categorized as either Aβ-dependent or Aβ-independent (37, 60). Aβ-dependent hypotheses arose from initial findings that identified apoE and Aβ interactions and thus position apoE as a contributor to the amyloid cascade (61, 62). Aβ-independent hypotheses center on apoE4 inherent instability and/or susceptibility to proteolysis which may contribute to neurotoxicity and neurodegeneration in AD (24, 60).

Aβ-*Dependent* Role of ApoE in AD Pathogenesis

The interaction between apoE and Aβ has been extensively characterized *in vitro* over the past decade and has led to several independent and somewhat controversial conclusions. Amino acids 244–272 of apoE and an Aβ peptide of amino acids 12–28 interact, and the resulting complex is SDS resistant and appears more quickly with apoE4 (48, 61, 63). ApoE accelerates Aβ fibrillization from a soluble state, with apoE4 binding and seeding fibrils more readily than apoE3 (64, 65). These initial studies established the first physical link between Aβ and apoE, lending support to the general view at the time that apoE4 accelerated Aβ deposition into plaques.

Since then, apoE4 has largely been hypothesized to act as a "pathological chaperone" that promotes the aggregation of Aβ or neurotoxic Aβ assembly states (47). The hydrophobic nature of the apoE lipid-binding domain has been proposed to act as a stabilizer of the Aβ fibril structure (9). However, despite the strong evidence of high-affinity interaction between apoE and Aβ *in vitro,* data from other studies have indicated a more complicated relationship between the two proteins. The source of apoE—purified human or recombinant versus that derived from cell cultures—may also affect the isoform-specific affinity between Aβ and apoE (66, 67). Alternatively, lipid-associated, cell-secreted apoE3 (and to a lesser extent, apoE4) binds Aβ preferentially, possibly to mediate its clearance rather than deposition (68).

Subsequently, animal studies with genetic models were used to explore the *in vivo* interactions between these two proteins. Transgenic mice overexpressing the human APP^{V717F} Indiana mutation displayed less Aβ deposition in the absence of apoE than

those with endogenous mouse apoE (69-71). These studies and others suggested that apoE facilitates plaque formation, confirming earlier *in vitro* data (48, 61). Interestingly, several recent papers reported a role for apoE-lipidation state as an important determinant for Aβ deposition. Deficiency of the intracellular cholesterol transporter ABCA1 decreases apoE levels in the CNS, leaves the remaining apoE poorly lipidated, and results in increased Aβ plaque deposition when bred to several different $hAPP_{FAD}$ transgenic mouse lines (72-74). Accordingly, these findings suggest *enhanced* interaction of poorly lipidated apoE with Aβ, leading to more plaque formation (72-74).

In contrast, transgenic mice expressing $hAPP^{V717F}$ and *human* apoE3 or apoE4 directed by a glial fibrillary acidic protein (GFAP) promoter on a mouse apoE knockout (mEKO) background had fewer Aβ deposits and neuritic dystrophy than $hAPP_{FAD}$/mEKO mice (75). These data suggested that human apoE mediates the clearance of Aβ, with apoE3 and apoE2 promoting clearance better than apoE4 (75, 76). This supported some of the earlier seemingly contradictory *in vitro* data, showing that apoE3 had a higher affinity for Aβ (67). Likewise, neuron-expressed human apoE3 or apoE4 on a mEKO background in $hAPP_{FAD}$ mice (line J9) also modified Aβ-related behavioral deficits and neuropathology in an isoform-dependent manner (13, 56). Generally, when co-expressed with $hAPP_{FAD}$ in mice, both apoE3 and apoE4, regardless of the cellular source (neurons or astrocytes), efficiently clear Aβ from the brain in young mice. However, at older ages, apoE4 mice have more Aβ deposits than apoE3 mice, again regardless of the cellular source of apoE (13, 76-78).

As such, the dual-role of apoE in AD pathology as a chaperone for Aβ deposition and/or clearance is complex. Either scenario implicates apoE in maintaining a

homeostatic balance of Aβ levels in the brain. More recently, apoE/Aβ interaction studies have begun to focus on small oligomeric Aβ assemblies, in addition to fibrillar deposits. A recent study has reported that apoE4 synergizes with oligomeric $A\beta_{42}$ to induce LTP impairment (79). Additionally, a 13-kDa C-terminal fragment of apoE (~amino acids 182–299) has been proposed to stabilize Aβ hexamers, supporting the hypothesis that increased levels of apoE fragments induce Aβ-related neurotoxicity (60, 80).

Based on these results, several strategies have been proposed for the development of Aβ-related anti-AD drugs. One strategy supports inhibiting the interaction of apoE with Aβ to prevent fibrillization (81, 82). Another favors the stimulation of apoE production and interaction with Aβ, especially apoE3 or apoE2 over apoE4, to support Aβ clearance (83). These two strategies propose different biological roles for apoE/Aβ interaction. For example, in a recent study, a non-fibrillogenic $A\beta_{12-28}$ peptide (conferred by a valine-to-proline substitution at residue 18) competitively inhibited the *in vivo* interaction of apoE with Aβ and subsequent plaque formation in $hAPP^{V717F}$ mice on a mouse apoE background (82). Levels of total Aβ, plaques, and cerebral amyloid angiopathy were decreased, and learning and memory were improved. The authors suggest that blocking the interaction of apoE with Aβ could be a promising therapeutic approach for AD. Conversely, another recent study tested the clearance hypothesis for human apoE through viral-mediated gene transfer of human apoE2 or apoE3 *in vivo*. Using the apoE-expressing lentivirus in $hAPP^{V717F}$ mice on a mEKO background, the authors found that expression of apoE3 decreased Aβ levels and reduced Aβ deposition (83). They also showed that expression of apoE4 under the same conditions promoted Aβ deposition and

increased soluble Aβ levels. The authors concluded by also suggesting that increasing apoE expression to further promote its interaction with Aβ might lead to enhanced Aβ clearance and prove to be beneficial to AD patients. Clearly, the basic questions about the mechanistic function of apoE and the nature of its interaction with Aβ (whether a negative or positive role) needs to be defined to aid in the development of anti-AD therapeutics targeting apoE.

Aβ-*Independent* Role of ApoE in AD Pathogenesis: ApoE Proteolysis Hypothesis

In addition to glial sources, apoE is produced by neurons during stress or brain injury, most likely to increase cholesterol transport, facilitate repair processes, and/or to protect neurons from further injury (24, 36, 60). Thus, the cellular source of apoE is an important factor, especially with recent data demonstrating neuron-specific proteolysis of apoE (29, 30). The proteolysis of apoE by an unknown chymotrypsin-like serine-protease occurs near the end of the lipid-binding domain (Leu-268 and/or Met-272), and yields C-terminal truncated fragments with a molecular mass of ~29 kDa, from which 14–20 kDa fragments can be further generated (29). Both lengths of fragments are neurotoxic *in vitro* and *in vivo* (28-30, 84). Increased proteolysis is observed in the brains of humans and transgenic mice with apoE4 more often than in those with apoE3 and is absent when the cellular source of apoE is purely from astrocytes (28-30, 85). Overall, apoE4 proteolysis reduces the level of full-length apoE, which may interfere with its normal cellular function.

These isoform-dependent cleavages may result from conformational differences between apoE3 and apoE4, such as the domain interaction that occurs in apoE4 but not in

apoE3 (86-88). Evidence for this comes from studies showing almost complete inhibition of apoE proteolytic cleavage *in vitro* when the residues necessary for domain interaction, Arg-61 and Glu-255, are mutated to Thr-61 or Ala-255 (37). In addition, domain interaction causes impaired intracellular trafficking of apoE4 from the ER to the Golgi apparatus in neuronal cells (89). Consequently, the retention of apoE4 in the ER or Golgi may increase its chance of proteolysis, misfolding, and degradation, further contributing to neuronal stress and toxicity (89).

These data thus support the hypothesis that a specific conformation of apoE at the lipid-binding domain determines an isoform-specific susceptibility to its dysfunction. Neuronal expression of apoE4 leads to its accumulation in the secretory pathway and increased susceptibility for proteolysis yielding neurotoxic fragments that may disrupt the cytoskeleton through tau hyperphosphorylation and impair mitochondria (24, 36, 37, 60). Accordingly, overexpression of the major apoE4 fragment in mice, truncated at amino acid 272–299 (apoE4Δ272–299), causes AD-like neuronal and behavioral deficits in transgenic mice expressing high levels of the fragment at young ages (6–7 months) (29) or with low levels of the fragment at old ages (12–13 months) (59).

Summary and Objectives

The apoE4 isoform confers increased risk for AD; however, the precise mechanism for its role remains unknown. Several theories place apoE4 in the amyloid cascade as a pathological chaperone to Aβ-related neurotoxicity or as an inherently unstable molecule prone to degradation and fragmentation. Either of these possibilities could be true and are not mutually exclusive. For instance, during aging, apoE fragments might accumulate

over time, thus reducing functional pools of apoE available for mediating Aβ clearance and leading to its simultaneous detrimental accumulation. Additionally, it is unknown whether these apoE fragments might synergize with Aβ or its various aggregated forms to exacerbate toxicity and neuronal impairments.

The objective of this study was to investigate the ability of C-terminal-truncated apoE4 to mediate Aβ clearance and to determine if C-terminal-truncated apoE4 synergizes with Aβ in eliciting neuronal and behavioral deficits. For this purpose, J20 $hAPP_{FAD}$ mice were cross-bred to apoE4(Δ272–299) transgenic mice, in which a major apoE4 fragment found in AD brains was expressed in neurons at low levels (29, 59). Since Aβ binds at the apoE C-terminus within the apoE lipid binding domain, the truncation of apoE in this region may impact its interaction with Aβ. Therefore, hippocampal Aβ levels and extent of deposition in the mice expressing either $hAPP_{FAD}$ alone, or with apoE4(Δ272–299), apoE3, or apoE4 were measured. Levels of calbindin, MAP2, and cFOS were also assessed to determine if apoE4(Δ272–299) synergized with Aβ toxicity to impair neuronal function. Elevated plus maze and Morris water maze behavioral tests were performed to determine if there were exacerbations in anxiety levels or learning and memory impairments.

CHAPTER 2

Materials and Methods

Reagents. Minimum essential medium, non-essential amino acids, penicillin/streptomycin, sodium pyruvate, and fetal bovine serum were from Invitrogen (Rockville, MD). Polyclonal goat anti-human apoE was from Calbiochem (San Diego, CA). Monoclonal 3D6 antibody against human Aβ was from Elan Pharmaceuticals (South San Francisco, CA). The anti-mouse and anti-goat IgG coupled to Alexa-488 or Alexa-594 was from Invitrogen. Horseradish peroxidase–coupled anti-mouse and anti-goat IgG were from Dako (Carpinteria, CA). ECL was from Amersham Biosciences (Arlington Heights, IL). Recombinant human apoE4 and apoE4(Δ272-299) were kindly provided by Dr. Karl Weisgraber (Gladstone Institute of Neurological Disease, San Francisco, CA). $A\beta_{42}$ peptide was from Biopeptides (San Diego, CA) and monomers were prepared as described (90).

Mice. J20 $hAPP_{FAD}$ mice express hAPP harboring the Swedish (K670N, M671L) and Indiana (V717F) mutations under the control of the PDGF promoter (12). These mice were backcrossed with murine apoE knockout mice (mEKO) and subsequently cross-bred with NSE-apoE3, NSE-apoE4, or Thy1-apoE4(Δ272–299) mice on the mEKO background. $hAPP_{FAD}$ mice with mouse apoE ($hAPP_{FAD}$/mE) were used in some analyses as controls. Similar numbers of male and female mice were studied at 6–8 months of age, except in behavioral experiments, in which female mice were studied at 5–9 months of age.

Tissue collection. Mouse brains were collected after deep anesthesia with avertin and transcardial perfusion with 0.9% saline. The left hemibrain was snap-frozen on dry ice; the right hemibrain was fixed in 4% paraformaldehyde for 48-h. After a 24-h rinse in phosphate-buffered saline (PBS), hemibrains were immersed in 30% sucrose/PBS and cut into 30-μm-thick sections on a Leica sliding microtome mounted with a freezing stage (Physitemp).

Aβ ELISA. Total Aβ ($Aβ_{(1-x)}$) and $Aβ_{42}$ levels in the hippocampus were measured by enzyme-linked immunosorbent assay (ELISA) as described (14). Briefly, snap-frozen hemibrains were thawed, and the hippocampi were dissected, weighed, and homogenized in 5 M guanidine buffer (10x volume/weight). Homogenates were spun at 14,000g for 20 min to pellet debris, serially diluted, and applied to plates coated with anti-$Aβ_{42}$ (clone 21F12) and anti-total-Aβ (clone m266) to detect Aβ peptides. The detection antibody was biotinylated anti-Aβ clone 3D6. All sample dilutions used to calculate Aβ levels were within the detection range based on a simultaneously generated standard curve.

ApoE and Aβ binding assay. Ninety-six-well plates were coated with $Aβ_{40}$ or $Aβ_{42}$ (330 ng/well) (Biopeptides), washed several times with washing buffer (PBS containing 0.05% Tween-20), and blocked overnight at 4°C with 4% bovine serum albumin in PBS. Subsequent incubations were performed at room temperature. The highest concentration of apoE4 or apoE4(Δ272–299) was 62.5 ng (18.1 nM) diluted in 100 μl of blocking buffer with fourfold dilutions thereafter. The mixture was applied to the Aβ-coated plate for 1-h, the plate was washed, and bound apoE was detected with a polyclonal anti-apoE antibody (Calbiochem). Anti-goat IgG labeled with horseradish peroxidase and TMBE

substrate (Thermo-Pierce) were sequentially applied, and the resulting signal was read at 450 nm on a SpectraMax M5 plate reader (Molecular Devices); data were collected with Softmax Pro. Each experiment was performed in duplicate and repeated three times. The detection of the apoE peptides by the polyclonal anti-apoE was determined to be comparable in a separate assay in which apoE4 or apoE4(Δ272–299) was coated at 50 ng/well onto a 96-well ELISA plate. Polyclonal anti-apoE was diluted serially starting at 1:4000 and fourfold thereafter and applied as the detection antibody by a protocol similar to above. Assay was performed in triplicates and repeated twice.

Immunohistochemistry, image collection, and quantitative analysis. Floating mouse brain sections (30 μm) were immunostained with mouse anti-human Aβ (clone 3D6, Elan Pharmaceuticals), goat anti-apoE (Calbiochem), mouse anti-MAP2 (SIGMA), rabbit anti-calbindin (Swant), and rabbit anti-Fos (Chemicon). Fluorescence was detected with donkey anti-goat Alexa Fluor 488, donkey anti-rabbit Alexa Fluor 488, and donkey anti-mouse Alexa Fluor 594 (Invitrogen). Signals were detected with biotinylated goat anti-rabbit IgG (Vector) or biotinylated donkey anti-mouse IgG (Jackson Immunoresearch Labs) and the ABC Elite detection kit (Vector Laboratories, Burlingame, CA) and diaminobenzidine (DAB). DAB-immunostained sections were analyzed for percent area occupied by plaques using Image J software (NIH). The optical density of calbindin immunoreactivity and the number of Fos-positive granule cells were quantified as described (14). To measure the levels of MAP2 immunoreactivity, images of four fluorescently immunostained sections (300 μm apart, starting at Bregma -1.6) from each mouse were collected with an epifluorescent upright microscope (Leica) using a 10x objective. Fluorescence intensities were quantified using Image J software (91).

Thioflavin S staining and quantification. Four serial sections (spaced 300 μm apart starting at Bregma –1.6) from each mouse were mounted onto Superfrost-plus slides (Fisher) and allowed to air-dry. After two rinses in PBS, the slides were incubated in 0.25% potassium permanganate for 5–10 min, washed three times in PBS, incubated in 2% $K_2O_5S_2$ and 1% oxalic acid for 5 min, washed three times in PBS, and stained with 0.015% Thioflavin S in 50% ethanol for 10 min. The slides were differentiated in 50% ethanol, rinsed with water and then PBS, and coverslipped. Quantification of Thioflavin S–positive plaques was performed manually using a 20x objective by an investigator blinded to the mouse genotypes. Data represent the average number of plaques per section in the hippocampal subfield of four sections per animal from 4–7 mice per genotype.

Morris water maze. A water maze pool with a diameter of 122 cm containing opaque water at 22–23°C was used with a platform 10 cm in diameter submerged 1.5 cm during hidden platform sessions (16, 29, 55). The platform base was switched to a black-and-white-striped mast (15 cm high) during cued training sessions. Mice were trained to locate the hidden platform for 5 days, in two daily sessions, each consisting of two 60-s trials 15 min apart. For the cued platform assessment, the mice were trained for 3 days in two daily sessions 3.5-h apart, each consisting of two 60-s trials with a 15-min intertrial interval. The platform location remained constant during the hidden platform sessions and was changed for each cued platform session. Entry points were changed semirandomly between trials. At 24-, 72-, and 120-h after the last hidden platform training, a 60-s probe trial (platform removed) was performed. Performance was monitored with an EthoVision video-tracking system (Noldus Information Technology).

Elevated plus maze. The elevated plus maze assesses anxiety in naive rodents by challenging them to decide between exploring a novel environment and anxiogenic elements such as elevation and a brightly illuminated area or hiding in safe, enclosed narrow space. The maze consists of two open arms and two closed arms equipped with rows of infrared photo-cells interfaced with a computer (Hamilton). Mice were placed individually into the center of the maze and allowed to explore for 10 min. The number of beam breaks was automatically recorded to calculate the amount of time spent, distance moved, and number of entries into the open or closed arms. Between tests, the maze was cleaned with 70% ethanol to standardize odors.

Detection of Aβ*56 oligomer. Snap frozen hemi-brains were slowly thawed on ice and dissected to isolate only the cortex and hippocampus. A four step-fractionation protocol was used as described (17). Briefly, the tissue was homogenized in 500 µl of NP40 lysis buffer (50 mM Tris-HCl, 0.01% NP40, 150 mM NaCl, 2 mM EDTA, 0.1% SDS) supplemented with PMSF, protease and phosphatase inhibitors (Sigma) and centrifuged at 3000g for 10 min at 4°C. The supernatant was collected and respun at 13000g for 90 min at 4ºC to obtain an extracellularly enriched fraction. The resulting pellet received 500 microliters of TNT buffer (50 mM Tris-HCl, 150 mM NaCl, 0.1% Triton X-100) with inhibitors, was vortexed vigorously and pipetted repeatedly to resuspend the pellet, and spun at 13000g for 90 min at 4°C to obtain the intracellular fraction. The final remaining pellet was resuspended in RIPA buffer (50 mM Tris-HCl, 0.5% Triton X-100, 150 mM NaCl, 1 mM EDTA, 3% SDS, 1% sodium deoxycholate) with inhibitors and respun at 26000rpm for 90 min at 4°C. The resulting supernatant was considered the membrane-bound fraction, assayed for total protein content by the bicinchoninic acid assay (BCA

kit, Pierce) and 500 μg of total protein was used for immunoprecipitation with 6E10 anti-Aβ (Signet). Lysates were eluted from the protein-G magnetic beads (Pierce), resolved by electrophoresis on 4–12% Bis/Tris Novex gels (Invitrogen), transferred to nitrocellulose membranes, and probed with biotinylated-6E10 (Signet, 1:2000).

Western blot. Snap frozen hemibrains that were not used for Aβ measurements were quickly thawed on ice, dissected to obtain the hippocampus, and homogenized in a low-detergent buffer (50 mM Tris pH 7.5, 150 mM sodium chloride, 1% NP-40, 0.5% sodium deoxycholate, 0.1% SDS, protease and phosphatase inhibitor cocktails). Homogenates were spun down at 30,000g for 30 min at 4ºC, and the supernatant was collected. All lysates were assayed for total protein concentrations with a BCA kit. Twenty micrograms of protein for each sample were loaded into 12% Bis/Tris Novex gels (Invitrogen) and run for 1-h at 200 mV. Proteins were transferred to nitrocellulose membranes and successful transfer was detected by Ponceau staining. Membranes were blocked for 1-h in 5% milk/TBS/0.5% Tween-20 and incubated with primary antibody (actin, apoE, APP) overnight at 4ºC in the same blocking buffer. Secondary antibody incubation was performed for 1-h at room temperature.

Statistical analysis. Values are expressed as mean ± SEM or SD. The statistical significance of differences between means was assessed by Student's *t* test or one-way ANOVA and Tukey-Kramer and Bonferroni *post hoc* tests (behavioral comparisons). Analysis of dissociation constants, Kd, was determined from a one-site binding non-linear regression equation. The differences in mouse survival were assessed by Kaplan Meier analysis.

CHAPTER 3

C-Terminal-Truncated Apolipoprotein E4 Inefficiently Clears Aβ Peptides and Acts in Concert with Aβ to Elicit Neuronal and Behavioral Deficits in Mice

Generation of $hAPP_{FAD}$ mice expressing human apoE3, apoE4, apoE4(Δ272–299), or mouse apoE. To determine the effect of the apoE4 fragment on Aβ levels in brains, transgenic mice expressing the C-terminal-truncated human apoE4 [apoE4(Δ272–299)] at low levels (29) were cross-bred with the J20 line of $hAPP_{FAD}$ mice (12). To avoid the potential combined effect of human and mouse apoE (mE), both parental lines were first bred onto the mouse apoE knockout (mEKO) background. The mice used in this study were $hAPP_{FAD}$/apoE4(Δ272–299)/mEKO, $hAPP_{FAD}$/mEKO, apoE4(Δ272–299)/mEKO, and mEKO. To generate $hAPP_{FAD}$/apoE3/mEKO and $hAPP_{FAD}$/apoE4/mEKO mice as additional controls, NSE-apoE3/mEKO and NSE-apoE4/mEKO mice (54) were crossed with $hAPP_{FAD}$/mEKO mice. $hAPP_{FAD}$ mice expressing endogenous mouse apoE ($hAPP_{FAD}$/mE) were also included in the study as additional controls. Expression of different forms of apoE at similar levels did not alter the levels of $hAPP_{FAD}$ in transgenic mice (Fig 1). To examine the potentially additive or synergistic effect of the apoE4 fragment with Aβ on neuronal and behavioral deficits, young $hAPP_{FAD}$ mice at 6–8 months of age were used, an age before extensive Aβ deposition occurs (12). The neuropathological studies focused on the hippocampus because it is preferentially affected in AD.

FIGURE 1

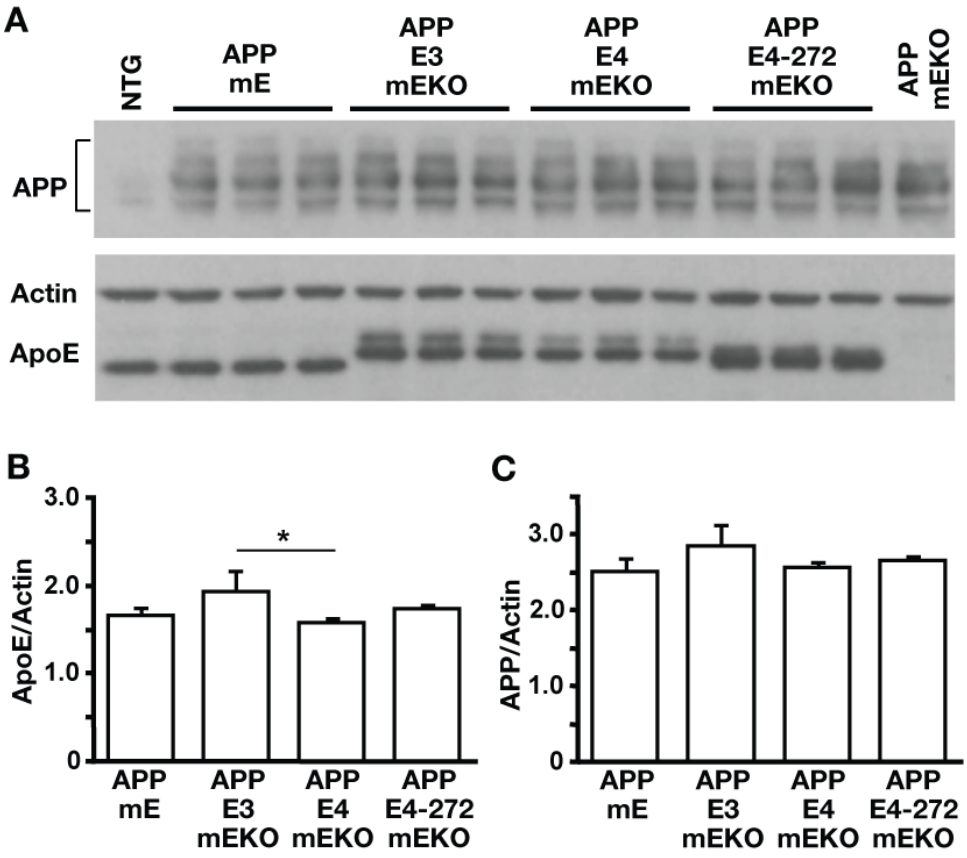

Figure 1. Expression levels of $hAPP_{FAD}$ and apoE in the hippocampus of different transgenic mice. ***A,*** Western blot analysis of full-length $hAPP_{FAD}$ (includes alternatively spliced isoforms APP695, APP751, and APP770), actin, and apoE in hippocampal lysates from different transgenic mice at 6–8 months of age. ***B,*** Ratios of apoE to actin in hippocampal lysates from different transgenic mice. ***C,*** Ratios of $hAPP_{FAD}$ to actin in hippocampal lysates from different transgenic mice. Values are mean ± SEM. n = 3 per genotype. *$*p < 0.05$* by one-way ANOVA with Tukey's *post-hoc* test. Abbreviations: NTG, nontransgenic; APP, $hAPP_{FAD}$; mEKO, mouse apoE knockout; E3, apoE3; E4, apoE4; E4-272, apoE4(Δ272–299).

Higher hippocampal Aβ levels in $hAPP_{FAD}$/apoE4(Δ272–299) mice than in $hAPP_{FAD}$ mice expressing apoE3 or apoE4. As determined by ELISA, $Aβ_{(1–x)}$ and $Aβ_{42}$ levels in the hippocampus were 94% lower in $hAPP_{FAD}$/apoE3/mEKO and 89% lower in $hAPP_{FAD}$/apoE4/mEKO mice than in $hAPP_{FAD}$/mEKO mice (Fig. 2*A*,*B*), consistent with the strong stimulation of Aβ clearance by apoE3 and apoE4 (13, 76-78). However, the $Aβ_{(1–x)}$ and $Aβ_{42}$ levels were significantly higher in $hAPP_{FAD}$/apoE4/mEKO than in $hAPP_{FAD}$/apoE3/mEKO mice, suggesting that apoE4 is less able to clear Aβ or has a higher tendency to retain Aβ than apoE3. Total Aβ and $Aβ_{42}$ levels were 3.5-fold and 6.8-fold higher in $hAPP_{FAD}$/apoE4(Δ272–299)/mEKO than in $hAPP_{FAD}$/apoE4/mEKO mice but 63% and 65% lower than in $hAPP_{FAD}$/mEKO mice (Fig. 2*A*,*B*). Thus, the apoE4 fragment is less able to clear Aβ or has a higher tendency to retain Aβ than the full-length apoE4. $hAPP_{FAD}$ mice with endogenous mouse apoE ($hAPP_{FAD}$/mE) had higher total Aβ levels than $hAPP_{FAD}$/mEKO mice and similar levels of $Aβ_{42}$, suggesting that mouse apoE does not significantly stimulate Aβ clearance or strongly retains Aβ in the brain.

The ratio of $Aβ_{42}$ to total Aβ is frequently used to indicate the fibrillogenic potential of a mixture of Aβ species (12). This ratio was about twofold higher in $hAPP_{FAD}$/apoE4(Δ272–299)/mEKO mice than in $hAPP_{FAD}$/apoE3/mEKO and $hAPP_{FAD}$/apoE4/mEKO mice, although significantly lower than in $hAPP_{FAD}$/mEKO mice (Fig. 2*C*). Thus, apoE4 fragment affects $Aβ_{42}$ clearance and/or retention more than full-length apoE3 and apoE4. The ratio of $Aβ_{42}$ to total Aβ was similar in $hAPP_{FAD}$/mE and $hAPP_{FAD}$/mEKO mice (Fig. 2*C*), suggesting that mouse apoE affects the clearance and/or retention of $Aβ_{42}$ and other Aβ species equally.

FIGURE 2

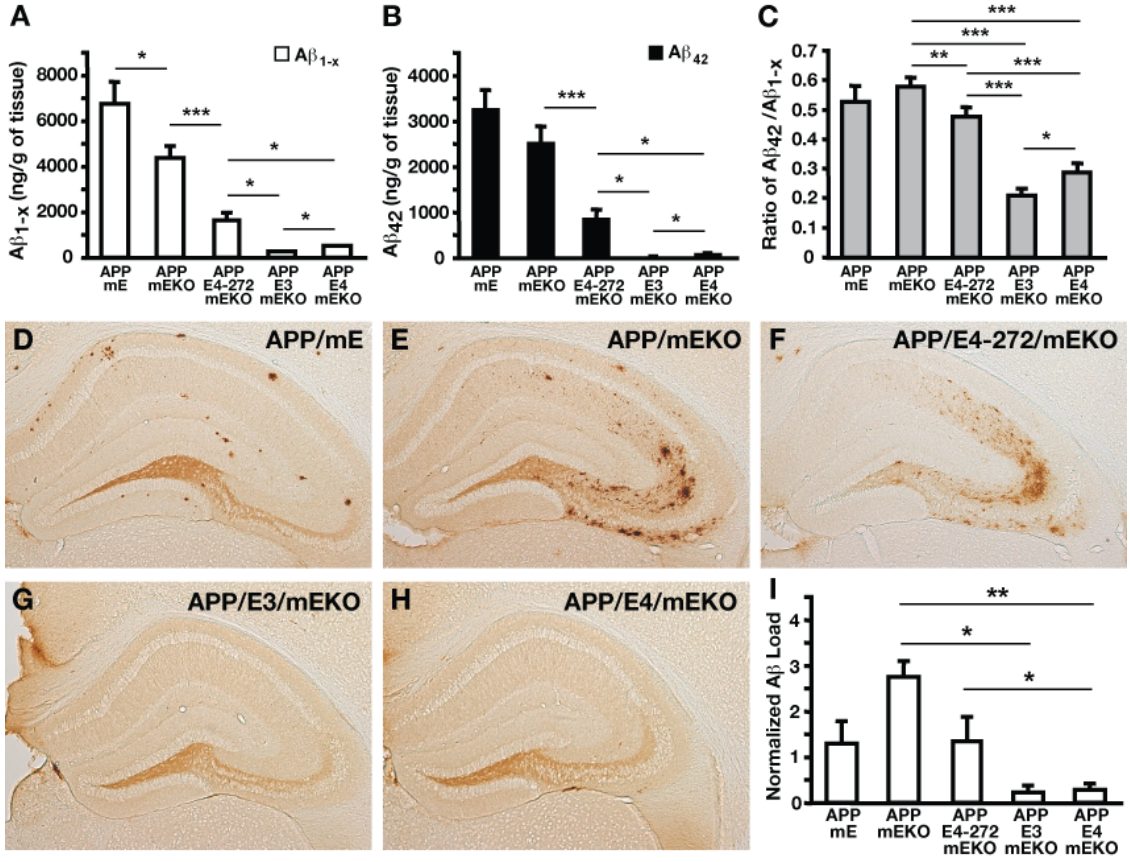

Figure 2. Aβ levels in the hippocampus of different mice at 6–8 months of age. ***A, B***, Levels of $A\beta_{1\text{-}x}$ (A) and $A\beta_{42}$ (B) were determined by a sandwich ELISA of hippocampal lysates homogenized in 5 M guanidine-HCl. ***C,*** $A\beta_{42}/A\beta_{1\text{-}x}$ ratios for each genotype. In A–C, values are mean ± SEM. n = 11–17 per genotype. *$p < 0.05$, **$p < 0.01$, ***$p < 0.001$ by Student's *t*-test for APP/mE versus APP/mEKO comparisons and one-way ANOVA with Tukey's *post hoc* test for all other comparisons. ***D–H***, Serial sections (30 μm thick collected 300 μm apart) from APP/mE (D), APP/mEKO (E), APP/E4-272/mEKO (F), APP/E3/mEKO (G), and APP/E4/mEKO (H) mice were immunostained with 3D6 monoclonal antibody. ***I,*** Percent area of Aβ deposition determined by densitometry. Values are mean ± SEM. n = 4–17 per genotype. *$p < 0.05$,

***p < 0.01* by one-way ANOVA with Tukey's *post hoc* test. Abbreviations: APP, $hAPP_{FAD}$; mE, mouse apoE; mEKO, mouse apoE knockout; E3, apoE3; E4, apoE4; E4-272, apoE4(Δ272–299).

Greater hippocampal Aβ deposition in $hAPP_{FAD}$/apoE4(Δ272–299) mice than in $hAPP_{FAD}$ mice expressing apoE3 or apoE4. To assess Aβ deposition, brain sections were immunostained with the 3D6 monoclonal antibody and the area of Aβ deposits in the hippocampus were quantified (12). Aβ accumulation in $hAPP_{FAD}$/apoE3/mEKO and $hAPP_{FAD}$/apoE4/mEKO mice was mostly in the hilus of the dentate gyrus (Fig. 2*G*,*H*) and only about 11% and 13% of the area, respectively, of those in $hAPP_{FAD}$/mEKO mice (Fig. 2*I*), which were more widespread (Fig. 2*E*), as reported (92). The Aβ deposits in $hAPP_{FAD}$/mE mice had dense cores (Fig. 2*D*) and were Thioflavin S–positive (Fig. 3A), while those in $hAPP_{FAD}$/mEKO mice were Thioflavin S–negative diffuse plaques (Fig. 2*E* and Fig. 3B). The area of Aβ deposition was fivefold greater in $hAPP_{FAD}$/apoE4(Δ272–299)/mEKO mice than in $hAPP_{FAD}$/apoE3/mEKO or $hAPP_{FAD}$/apoE4/mEKO mice (Fig. 2*I*). The location and morphology of Aβ deposits were similar in $hAPP_{FAD}$/apoE4(Δ272–299)/mEKO mice and $hAPP_{FAD}$/mEKO mice (Fig. 2*E*,*F*), although the area was 46% smaller in $hAPP_{FAD}$/apoE4(Δ272–299)/mEKO mice (Fig. 2*I*). There were no Thioflavin S–positive plaques in $hAPP_{FAD}$/apoE4(Δ272–299)/mEKO mice (Fig. 3C). Thus, mouse apoE stimulated dense-core plaque formation (92), while human apoE4 fragment led to more diffuse Aβ accumulation in the brain parenchyma.

FIGURE 3

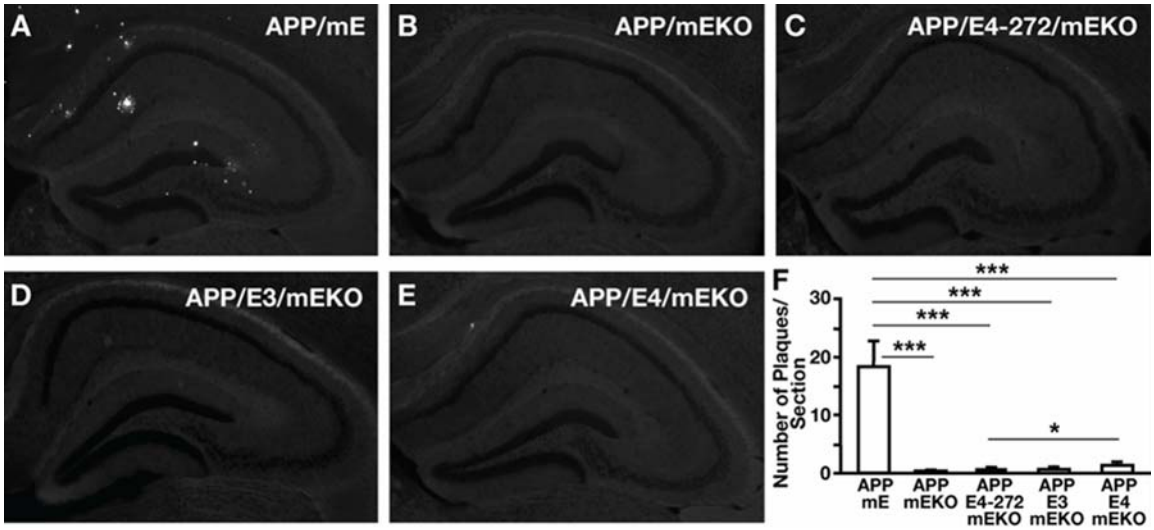

Figure 3. Thioflavin S staining of hippocampal sections from different transgenic mice. ***A–E***, Serial sections from APP/mE (A), APP/mEKO (B), APP/E4-272/mEKO (C), APP/E3/mEKO (D), and APP/E4/mEKO (E) mice were stained with Thioflavin S. ***F,*** Quantification of the average number of Thioflavin S–positive plaques per section. Values are mean ± SEM. n = 4–9 per genotype. *$p < 0.05$, ***$p < 0.001$ by one-way ANOVA with Tukey's *post hoc* test. Abbreviations: APP, $hAPP_{FAD}$, mE, mouse apoE; mEKO, mouse apoE knockout; E3, apoE3; E4, apoE4; E4-272, apoE4(Δ272–299).

ApoE4(Δ272–299) is not present in Aβ deposits and has a lower binding affinity for Aβ than apoE4. Double immunofluorescence staining for apoE and Aβ revealed that apoE3 and apoE4 localized within Aβ deposits in the dentate gyrus of the hippocampus in $hAPP_{FAD}$/apoE3/mEKO and $hAPP_{FAD}$/apoE4/mEKO mice (Fig. 4*B,C*). In $hAPP_{FAD}$/mEKO mice, as expected, there was no apoE staining in neurons or Aβ deposits (Fig. 4*A*). Surprisingly, apoE4(Δ272–299) was not detected within any Aβ deposits in the CA1, CA3, and dentate gyrus of $hAPP_{FAD}$/apoE4(Δ272–299)/mEKO mice (Fig. 4*D–F*). Thus, apoE4(Δ272–299) may not interact as effectively with Aβ *in vivo* as apoE3 and apoE4.

To test this possibility, an *in vitro* binding assay was performed in which different forms of apoE were incubated in 96-well plates coated with Aβ peptides. Although the apoE detection antibody had equal affinities for apoE4 and apoE4(Δ272–299) (Fig. 4*I*), apoE4(Δ272–299) bound less well to $Aβ_{40}$ and $Aβ_{42}$, compared to apoE4 (Fig. 4*G,H*), suggesting that the C-terminal region of apoE (aa 272–299) is critical for its interaction with Aβ. Thus, the higher Aβ levels in $hAPP_{FAD}$/apoE4(Δ272–299)/mEKO mice than in $hAPP_{FAD}$/apoE4/mEKO mice (Fig. 2*A,B*) are likely due to the decreased ability of apoE4(Δ272–299) to bind with Aβ, contributing to impaired Aβ clearance.

FIGURE 4

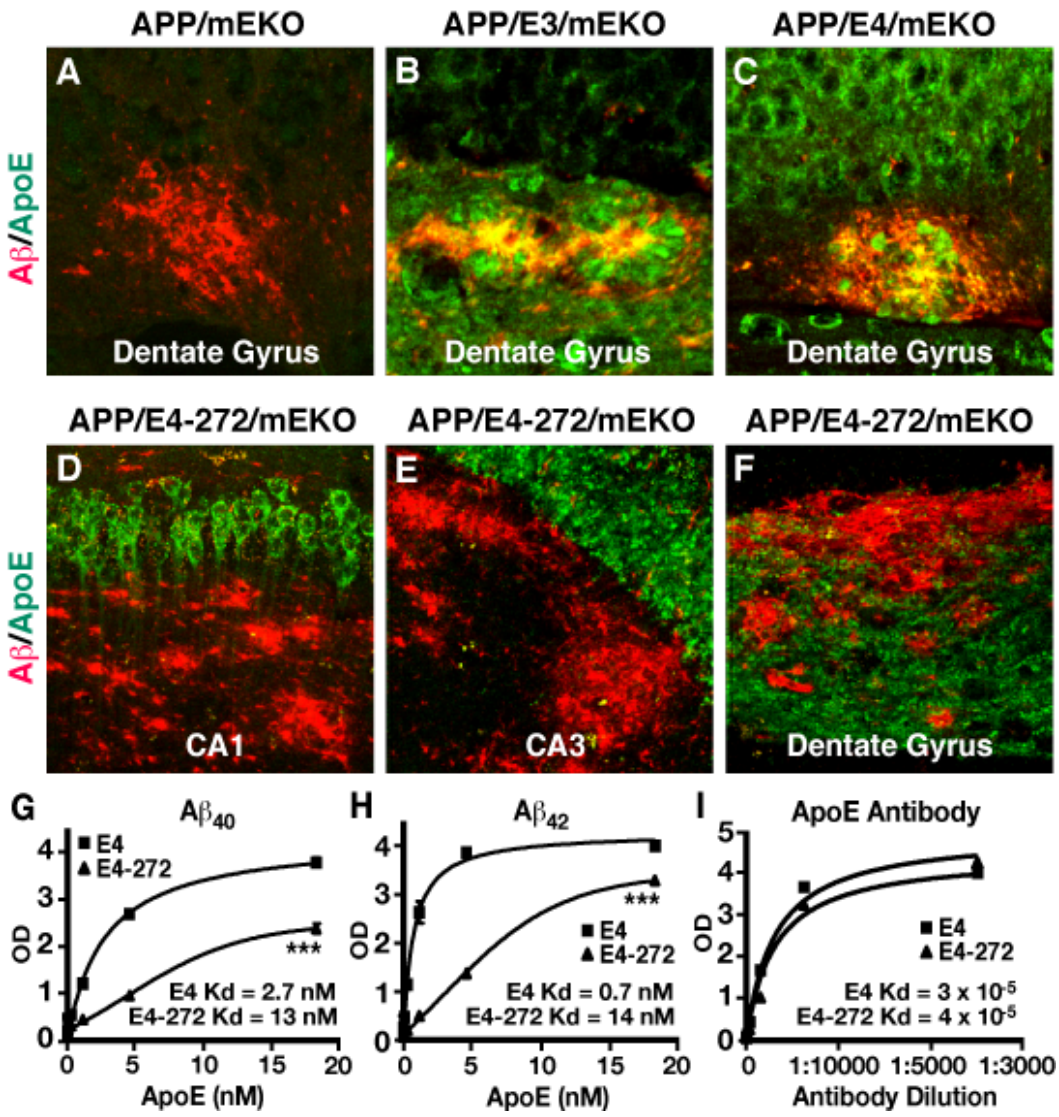

Figure 4. Fluorescence immunostaining for Aβ and apoE in the hippocampus of different mice at 6–8 months of age. ***A***, ApoE immunoreactivity is absent in APP/mEKO mice. ***B***, ***C***, ApoE colocalizes with Aβ in Aβ deposits in $hAPP_{FAD}$ mice expressing apoE3 (B) or apoE4 (C). ***D–F***, The apoE4 fragment does not colocalize with Aβ in $hAPP_{FAD}$ mice expressing apoE4-272. ***G***, ***H***, Aβ interaction with apoE4 or apoE4-272 detected by

ELISA. $A\beta_{40}$ (G) or $A\beta_{42}$ (H) was coated onto 96-well microtiter plates (330 ng/well) and allowed to bind to decreasing concentrations of recombinant apoE4 or apoE4-272 (starting amount was 62.5 ng with fourfold dilutions thereafter). Bound apoE was detected with a polyclonal apoE antibody. ***I,*** The polyclonal anti-apoE reacts equally well with apoE4 and apoE4-272 in an ELISA. ApoE4 or apoE4-272 was coated at 50 ng/well onto a 96-well ELISA plate. Polyclonal anti-apoE was diluted serially starting at 1:4000 and fourfold thereafter and applied as the detection antibody. Data points are mean ± SD. ****p < 0.001* for differences assessed by a one-site binding non-linear regression equation.

ApoE4 fragment acts in concert with Aβ to elicit neuronal deficits in mice. To next determine if the apoE4 fragment and Aβ act in concert to elicit neuronal deficits, an immunostaining was performed for MAP2, a dendritic marker (54). ApoE4(Δ272–299)/mEKO mice, which had no Aβ accumulation in the hippocampus, showed a trend toward lower MAP2 immunoreactivity (IR) in the hilus and molecular layer of the dentate gyrus than mEKO mice (Fig. 5*A,B,E,F*), which had similar MAP2 IR to apoE3 transgenic mice, as reported (93). $hAPP_{FAD}$/mEKO mice, which had high levels of Aβ in the hippocampus (Fig. 2*A,B,E,I*), had a significant reduction in MAP2 IR in the hilus and molecular layer of the dentate gyrus (Fig. 5*A,C,E,F*).

Importantly, the MAP2 reduction in both areas was similar in $hAPP_{FAD}$/apoE4(Δ272–299)/mEKO mice, which had 63% lower Aβ levels and 46% less Aβ deposition than $hAPP_{FAD}$/mEKO mice (Fig. 2*A,B,F,I*), and in $hAPP_{FAD}$/mEKO mice (Fig. 5*C,D,E,F*). There was no significant difference in MAP2 IR in the CA1 area of the hippocampus among the various groups of mice (Fig. 5*G*). Thus, the apoE4 fragment appears to have enhanced toxicity in the presence of low levels of Aβ to cause a pronounced decrease in MAP2 levels, probably a reflection of dendritic impairment specifically in the hilus and molecular layer of the dentate gyrus. Interestingly, the premature death of $hAPP_{FAD}$ mice, as reported (16, 29, 55), was also similar in $hAPP_{FAD}$/mEKO and $hAPP_{FAD}$/apoE4(Δ272–299)/mEKO mice (Fig. 5*H*), although the latter had significantly lower Aβ levels and Aβ deposition. These findings support the possibility that the toxicity of the apoE4 fragment is further increased *in vivo* in the presence of low levels of Aβ and may contribute to the early mortality observed in the mice.

FIGURE 5

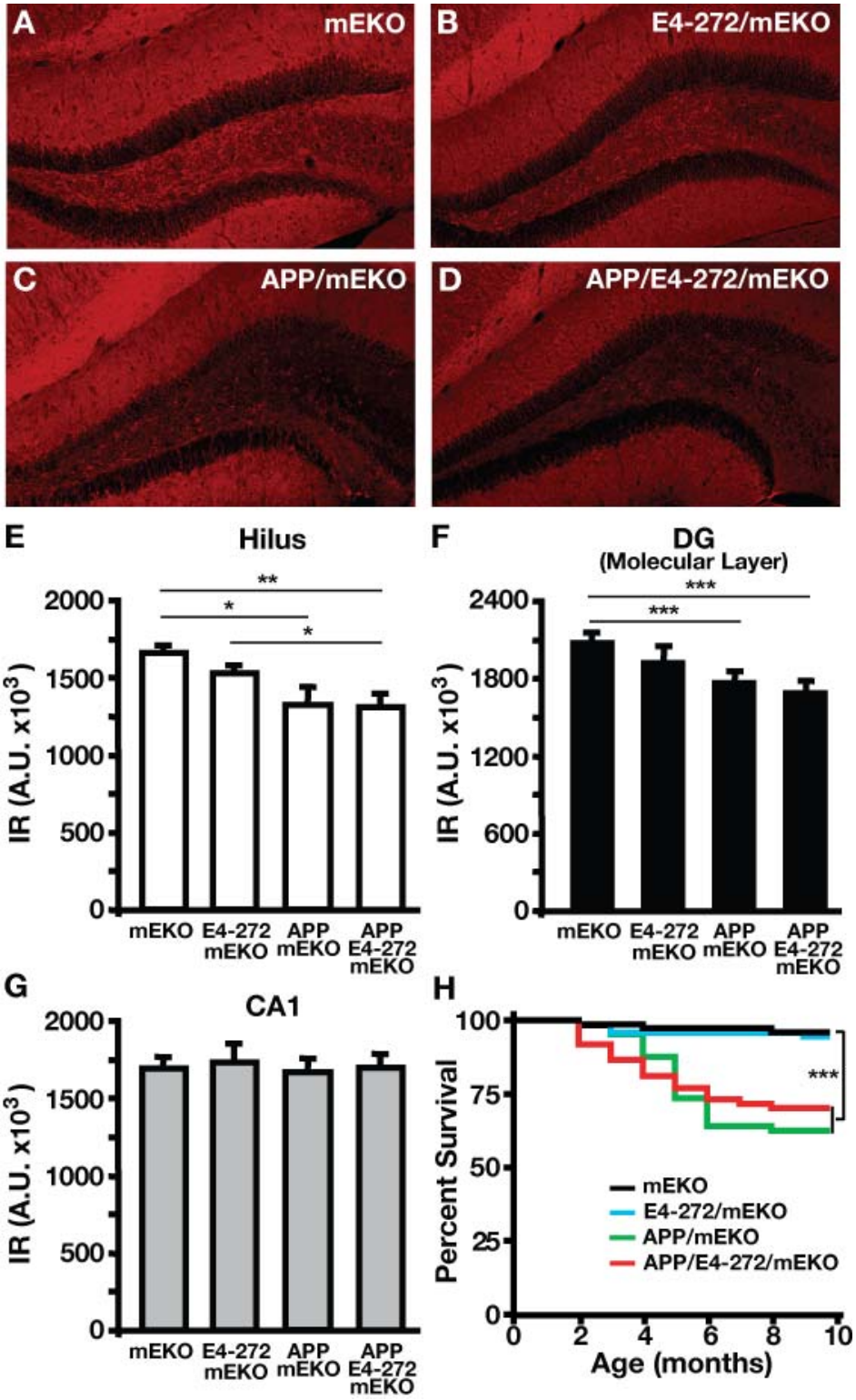
A
mEKO
B
E4-272/mEKO
C
APP/mEKO
D
APP/E4-272/mEKO
E
Hilus
IR (A.U. x10³)
2000
1500
1000
500
0
**
*
*
mEKO
E4-272 mEKO
APP mEKO
APP E4-272 mEKO
F
DG
(Molecular Layer)
IR (A.U. x10³)
2400
1800
1200
600
0
***
***
mEKO
E4-272 mEKO
APP mEKO
APP E4-272 mEKO
G
CA1
IR (A.U. x10³)
2000
1500
1000
500
0
mEKO
E4-272 mEKO
APP mEKO
APP E4-272 mEKO
H
Percent Survival
100
75
50
25
0
***
mEKO
E4-272/mEKO
APP/mEKO
APP/E4-272/mEKO
0
2
4
6
8
10
Age (months)

Figure 5. Immunostaining of MAP2 in different mice at 6–8 months of age. ***A–D,*** MAP2 staining in representative sections from mEKO (A), E4-272/mEKO (B), APP/mEKO (C), and APP/E4-272/mEKO (D) mice. ***E–G,*** MAP2 IR determined by densitometry in the hilus (E), the molecular layer of the dentate gyrus (DG) (F), and the CA1 region (G) of the hippocampus. Values are mean ± SEM. n = 7–22 per genotype. $*p < 0.05$, $**p < 0.01$, $***p < 0.001$ by one-way ANOVA with Tukey's *post hoc* test. ***H,*** The differences in mouse survival were assessed by Kaplan Meier analysis. n = 73 for mEKO, n = 92 for E4-272/mEKO, n = 64 for APP/mEKO, n = 74 for APP/E4-272/mEKO; $***p < 0.001$. IR, immunoreactivity; A.U., arbitrary units.

Immunostaining was also performed for calbindin, an activity-dependent calcium binding protein that is significantly decreased in the dentate gyrus of mouse models of AD and whose levels correlate with cognitive impairment (14). ApoE4(Δ272–299)/mEKO mice, which had no Aβ accumulation in the hippocampus, displayed moderately less calbindin IR in the molecular layer of the dentate gyrus than mEKO mice (Fig. 6*A,B,E*). $hAPP_{FAD}$/mEKO mice, which had high levels of Aβ in the hippocampus (Fig. 2*A,B,E,I*), had a greater reduction in calbindin IR (Fig. 6*A,C,E*). Importantly, the calbindin reduction was similar in $hAPP_{FAD}$/apoE4(Δ272–299)/mEKO mice, which had 63% lower Aβ levels and 46% less Aβ deposition than $hAPP_{FAD}$/mEKO mice (Fig. 2*A,B,F,I*), and in $hAPP_{FAD}$/mEKO mice (Fig. 6*C,D,E*). Thus, the apoE4 fragment may be more toxic in the presence of low levels of Aβ, leading to a pronounced decrease in calbindin levels. Furthermore, $hAPP_{FAD}$/apoE4(Δ272–299)/mEKO mice had significantly reduced calbindin IR in the CA1 stratum radiatum layer of the hippocampus, unlike mice

expressing either apoE4(Δ272–299) or $hAPP_{FAD}$ alone (Fig. 6*F*), supporting a possible synergistic effect of the apoE4 fragment and Aβ in this subregion.

FIGURE 6

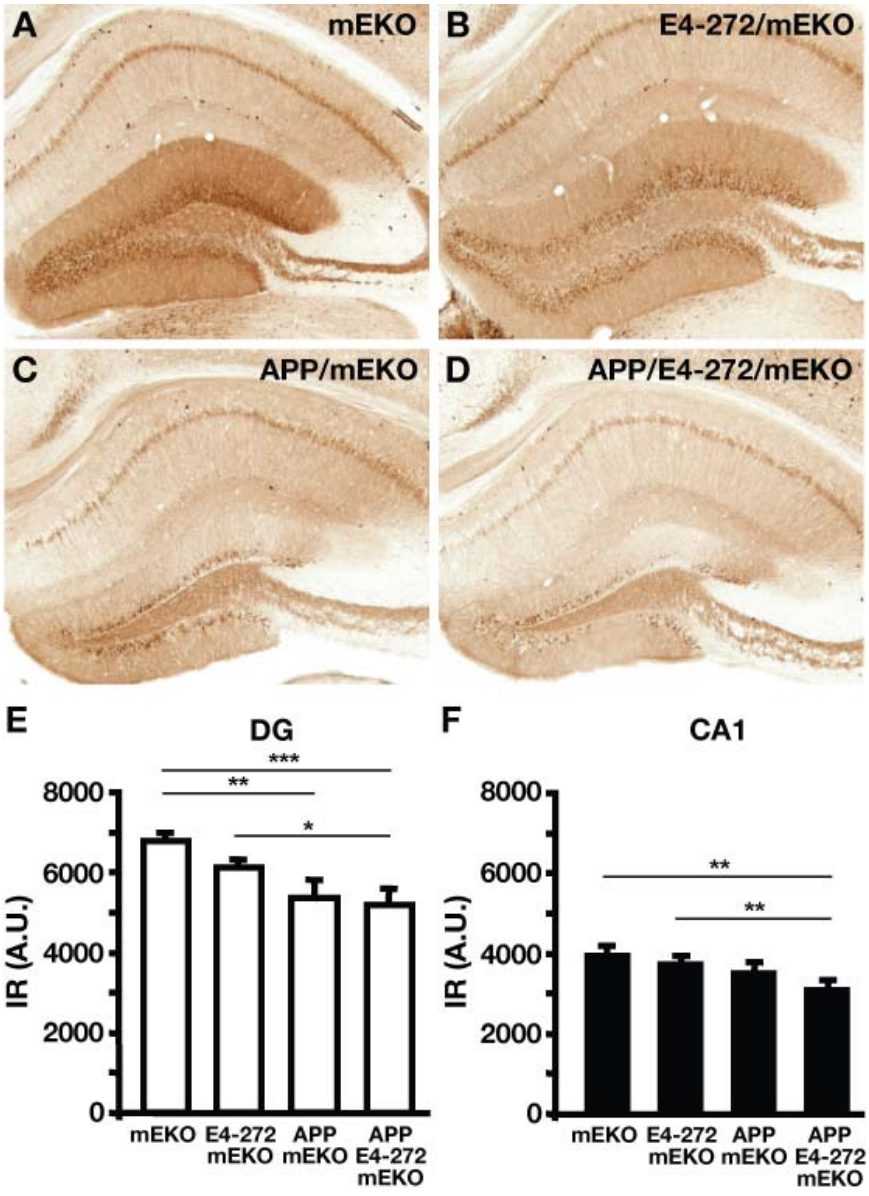

Figure 6. Immunostaining of calbindin in different mice at 6–8 months of age. ***A–D***, Calbindin staining in representative sections from mEKO (A), E4-272/mEKO (B), APP/mEKO (C), and APP/E4-272/mEKO (D) mice. ***E, F,*** Calbindin IR determined by densitometry in the dentate gyrus (E) and the CA1 region (F) of the hippocampus. Values are mean ± SEM. n = 7–22 per genotype. *$*p < 0.05$, **$p < 0.01$, ***$p < 0.001$* by one-way ANOVA with Tukey's *post hoc* test. IR, immunoreactivity; A.U., arbitrary units.

The granule cells of the dentate gyrus were analyzed for expression of Fos, an immediate-early gene encoding a synaptic activity-dependent protein. A reduction in the number of Fos-positive granule cells may indicate neuronal impairment and/or decreased synaptic activation (14). $hAPP_{FAD}$/mEKO mice, which had high levels of Aβ accumulation, and $hAPP_{FAD}$ mice expressing apoE4(Δ272–299), which had significantly lower Aβ accumulation, had similar reductions in the number of Fos-positive granule cells to levels much lower than those in mice not expressing any apoE or only apoE4(Δ272–299) (Fig. 7). Thus, activity-dependent Fos transcription was significantly reduced in the presence of apoE4 fragments and/or Aβ. The decrease in the number of Fos-expressing neurons may be attributed to toxicity of Aβ alone in the $hAPP_{FAD}$/mEKO mice, or due to enhanced toxicity of the apoE4 fragment when combined with low levels of Aβ in $hAPP_{FAD}$ mice expressing apoE4(Δ272–299). Furthermore, these reductions in Fos-positive neurons suggest that apoE4 fragment and Aβ may either impair the signaling pathways that induce Fos expression in response to neuronal activation or cause general synaptic dysfunction in these neuronal populations.

FIGURE 7

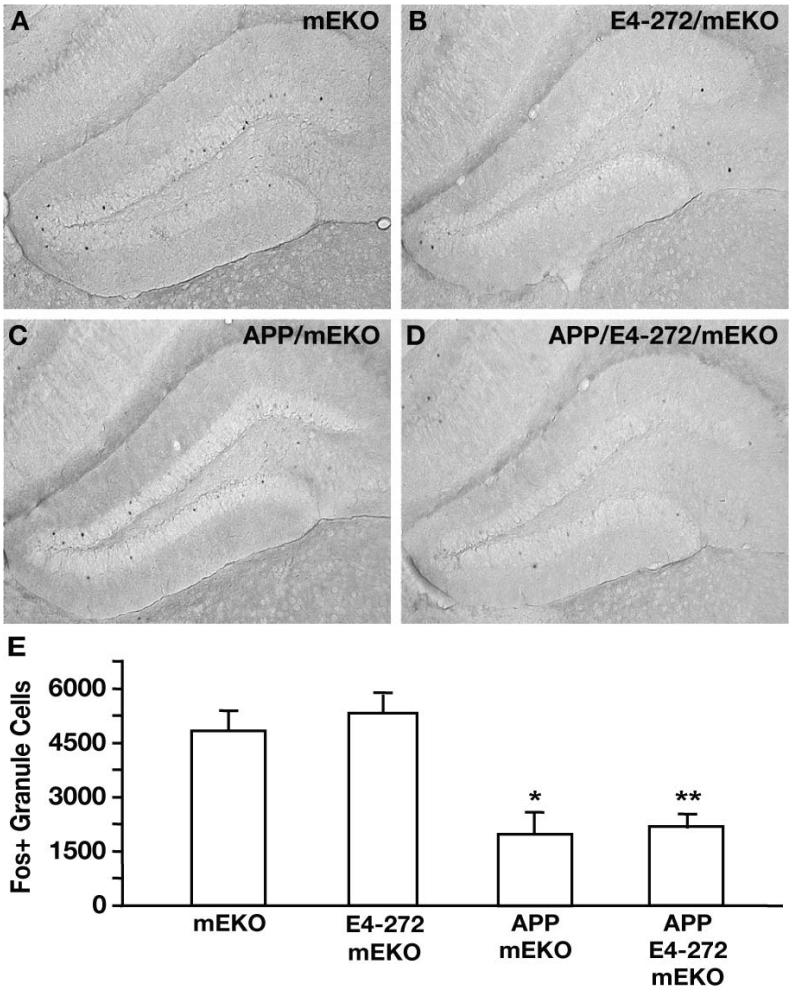

Figure 7. Immunostaining of Fos in the dentate gyrus of different mice at 6–8 months of age. ***A–D,*** Representative anti-Fos images from mEKO (A), E4-272/mEKO (B), APP/mEKO (C), and APP/E4-272/mEKO (D) mice. ***E,*** Quantification of Fos-positive granule cells in the dentate gyrus of different mice. Values are mean ± SEM. n = 7–22 per genotype. *$p < 0.05$ versus mEKO mice and **$p < 0.01$ versus E4-272/mEKO by one-way ANOVA with Tukey's *post hoc* test. Abbreviations: APP, $hAPP_{FAD}$; mEKO, mouse apoE knockout; E4-272, apoE4(Δ272–299).

ApoE4 fragment acts in concert with Aβ to elicit behavioral deficits in mice. To next determine if the apoE4 fragment and Aβ act in concert to induce behavioral deficits, spatial learning and memory were assessed by the Morris water maze test. At 5–9 months of age, mEKO mice quickly learned to find the hidden platform (Fig. 8*A*). At this age, mEKO mice learn as well as wildtype mice in the Morris water maze (94). However, $hAPP_{FAD}$/mEKO mice showed a mild, but significant deficit in spatial learning (Fig. 8*A*). ApoE4(Δ272–299)/mEKO mice did not differ significantly from mEKO mice in the hidden platform trial at this young age (Fig. 8*A*). $hAPP_{FAD}$/apoE4(Δ272–299)/mEKO and $hAPP_{FAD}$/mEKO mice had similar impairments in spatial learning (Fig. 8*A*), although the former had 63% lower Aβ levels and 46% less Aβ deposition (Fig. 2*A,B,I*). Swim speeds did not differ among various groups (Fig. 8*D*), indicating that the impairment was not due to motor deficits. All mice performed equally well in visible platform trials (Fig. 8*A*). In the probe trials, 72 h (Fig. 8*B*) and 120 h (Fig. 8*C*) after the last hidden platform trial, $hAPP_{FAD}$/apoE4(Δ272–299)/mEKO mice had impaired memory retention, while apoE4(Δ272–299)/mEKO and $hAPP_{FAD}$/mEKO mice did not (Fig. 8*B,C*), suggesting a concerted or synergistic detrimental effect of apoE4 fragment and Aβ on memory retention.

In the elevated plus maze, both mEKO and apoE4(Δ272–299)/mEKO mice had normal levels of anxiety at 5–9 months of age (Fig. 9). However, abnormalities in anxiety were observed in $hAPP_{FAD}$/mEKO mice and further increased in $hAPP_{FAD}$/apoE4(Δ272–299)/mEKO mice (Fig. 9).

FIGURE 8

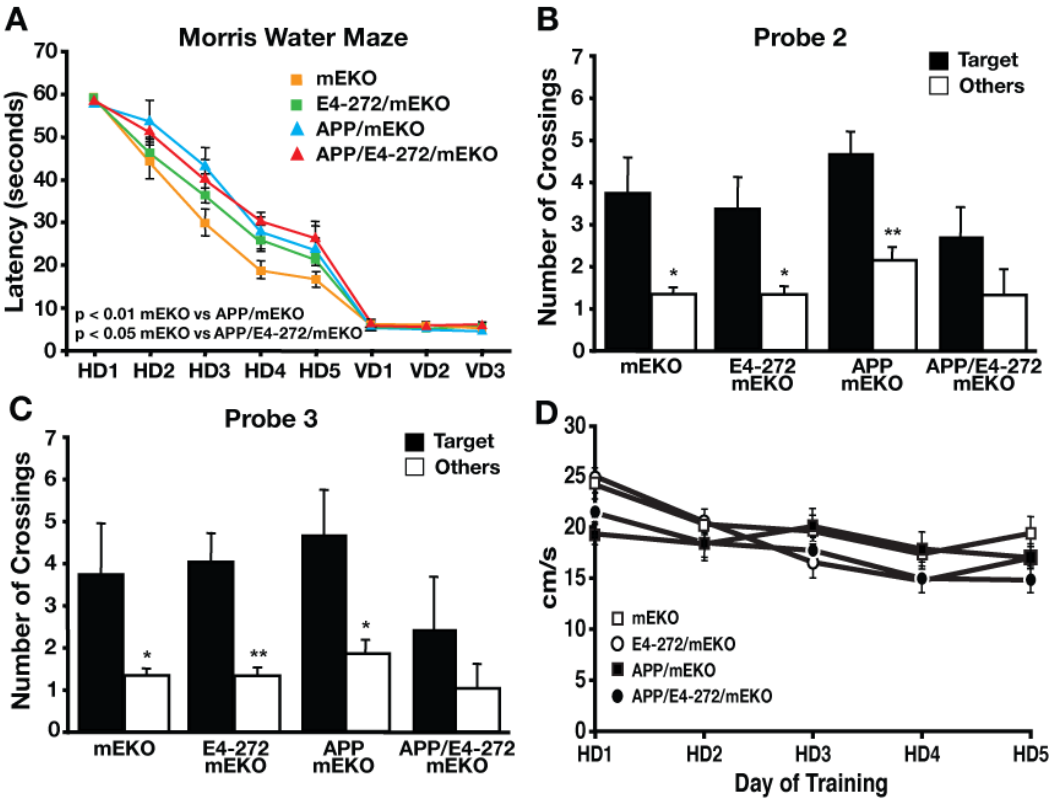

Figure 8. Learning and memory impairments and abnormal anxiety in $hAPP_{FAD}$ mice expressing apoE4(Δ272–299). ***A–C***, Spatial learning and memory were tested in the Morris water maze in female mice at 5–9 months of age. ***A***, Learning curves for the hidden portion of the water maze. Repeated measures ANOVA and Tukey/Bonferroni multiple comparison tests were performed for the learning curves across hidden days 1–5. ***B, C***, Memory in probe trials 72 h (B) and 120 h (C) after the last session of the hidden platform trial. ***D***, No difference in swim speeds during the hidden platform trials in the Morris water maze among mEKO, E4-272/mEKO, APP/mEKO, and APP/E4-272/mEKO mice. Values are mean ± SEM. n = 6–10 per genotype. $*p < 0.05$, $**p < 0.01$ for platform crossings versus average of crossings over the equivalent position of the

platform in the other three quadrants by Student's *t* test, and for the learning curves by ANOVA with Tukey/Bonferroni post-hoc comparisons; HD, hidden day; VD, visible day. Abbreviations: APP, $hAPP_{FAD}$; mEKO, mouse apoE knockout; E4-272, apoE4(Δ272–299).

FIGURE 9

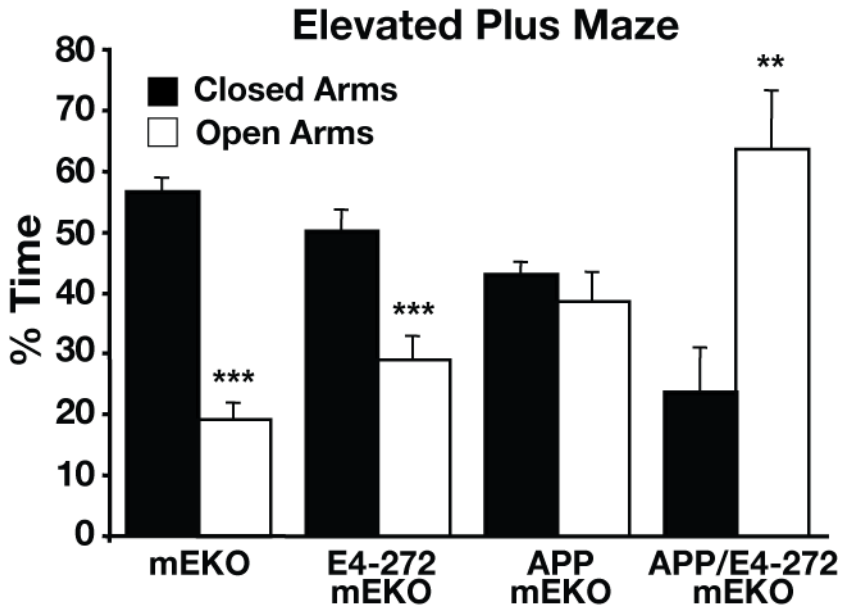

Figure 9. Anxiety was assessed in the elevated plus maze test. mEKO and E4-272/mEKO mice preferred the closed arms of the elevated plus maze significantly more than the open arms. APP/mEKO mice did not show a preference. APP/E4-272/mEKO mice spent significantly more time in the open arms of the elevated plus maze. Values are mean ± SEM. n = 6–10 per genotype. $^{**}p < 0.01$, $^{***}p < 0.001$ for percent time spent in closed arms versus open arms by Student's *t* test. Abbreviations: APP, $hAPP_{FAD}$; mEKO, mouse apoE knockout; E4-272, apoE4(Δ272–299).

Accumulation of pathogenic Aβ oligomers in $hAPP_{FAD}$/apoE4(Δ272–299)/mEKO mice with low levels of total Aβ. In searching for mechanisms underlying the concerted effects of apoE4 fragment and low levels of Aβ on neuronal and behavioral deficits, the levels of Aβ*56, a putative pathogenic Aβ oligomer species that correlates with learning and memory deficits in different lines of $hAPP_{FAD}$ mice, were measured (17, 19, 95). Aβ*56 isolated from $hAPP_{FAD}$ mouse brains also elicits memory deficits when injected into the brains of wildtype rats (17). Interestingly, $hAPP_{FAD}$/apoE4(Δ272–299)/mEKO mice had a trend toward significantly greater Aβ*56 levels (p = 0.05) than $hAPP_{FAD}$/mEKO mice (Fig. 10*B*), although the former had 63% lower Aβ levels (Fig. 2*A*,*B*). The overall total hAPP levels were comparable in the two groups of mice (Fig. 1 and 10). Thus, apoE4 fragments inefficiently clear Aβ peptides, which may result in the enhanced formation and/or accumulation of Aβ*56 to possibly contribute to the development of neuronal and behavioral deficits.

FIGURE 10

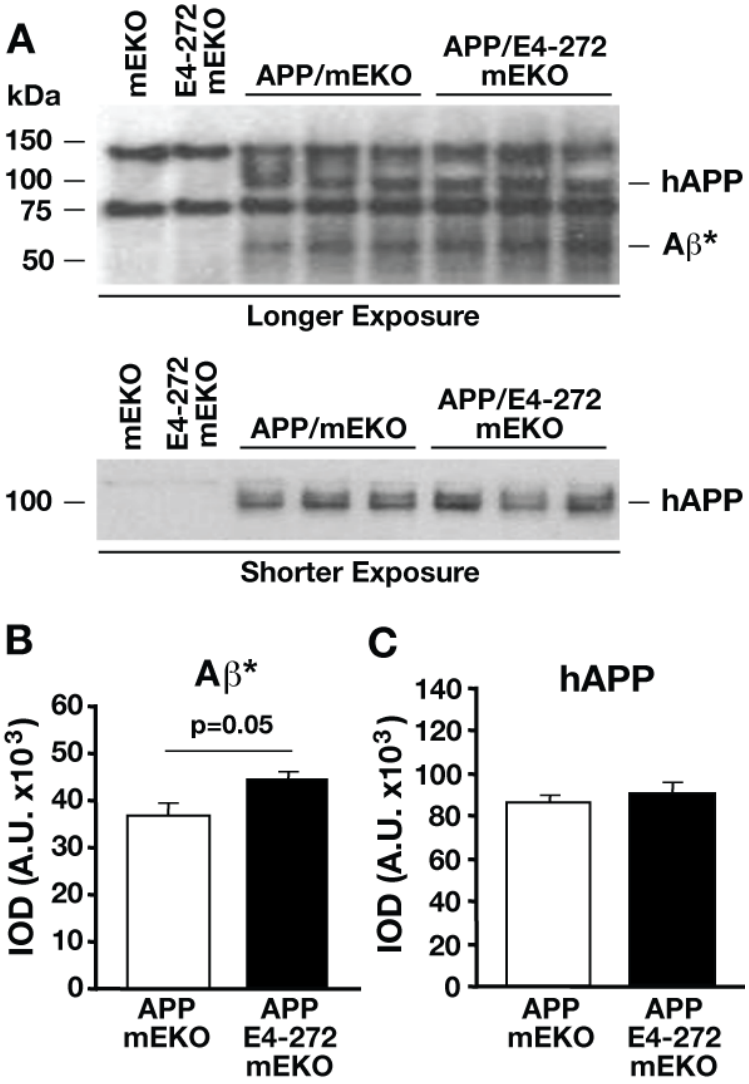

Figure 10. Accumulation of Aβ oligomers in the hippocampus of $hAPP_{FAD}$/apoE4(Δ272–299)/mEKO mice with low levels of total Aβ. ***A***, Western blot analysis of Aβ*56 and full-length hAPP. ***B***, Quantification of Aβ*56. ***C***, Quantification of hAPP. Values are mean ± SEM. n = 3 per genotype. *p*-value obtained by Student's *t* test. Abbreviations: APP, $hAPP_{FAD}$; mEKO, mouse apoE knockout; E4-272, apoE4(Δ272–299); IOD, integrated optical density; A.U., arbitrary units.

CHAPTER 4

Conclusions and Discussion

This study shows that $hAPP_{FAD}$/apoE4(Δ272–299)/mEKO mice had much higher levels of total Aβ and $Aβ_{42}$ and more Aβ deposits than $hAPP_{FAD}$/apoE3/mEKO and $hAPP_{FAD}$/apoE4/mEKO mice at 6–8 months of age. ApoE4(Δ272–299) did not colocalize with Aβ in deposits and had a lower binding affinity for $Aβ_{42}$ and $Aβ_{40}$. Thus, it likely has less ability to clear Aβ than full-length apoE3 and apoE4, rather than a greater tendency to stimulate Aβ deposition. Furthermore, the C-terminal-truncated apoE4 fragment acts in concert with lower levels of Aβ to elicit neuronal and behavioral deficits in mice at 5–9 months of age. Thus, apoE4 fragments and Aβ may act in concert to contribute to AD pathogenesis.

Importantly, these data demonstrate for the first time that the C-terminal 28 amino acids (aa 272–299) in apoE are critical in mediating its interaction with Aβ and thus in Aβ clearance, at least in mice. ApoE has two structural domains—an amino-terminal domain (aa 1–191) containing the receptor binding region (aa 135–150) and a carboxyl-terminal domain (aa 222–299) containing the lipid binding region (aa 241–272), which are linked by a hinge region (aa 192–221) (26). *In vitro* studies of the interaction between apoE and Aβ identified the lipid-binding domain as the binding partner for Aβ peptides (61, 63). These findings suggest that the C-terminal 28 amino acids (aa 272–299) affect the conformation of this domain, altering its interaction with Aβ. In agreement with this possibility, biophysical studies suggest that the lipid-binding domain has a less organized structure in C-terminal-truncated apoE4 than in apoE4 (96, 97). In addition, C-terminal-

truncated apoE4 fragments are more abundant in AD brains than in age-matched controls (28, 29). Others reported lower levels of apoE4 in AD brains than in controls (98). Thus, an increase in the ratio of C-terminal-truncated apoE4 to apoE4, which conveys a decreased ability to clear Aβ, might contribute to increased Aβ accumulation and plaque formation in AD patients with apoE4.

The data confirm that both apoE3 and apoE4 stimulate Aβ clearance in young mice, while mouse apoE stimulates more Aβ deposition than the absence of apoE (92). This observation has implications for understanding the effect of apoE on Aβ metabolism and for validating and interpreting clinical trials of anti-Aβ therapy. Almost all preclinical drug development studies related to Aβ are performed in $hAPP_{FAD}$ mice with mouse apoE (99). If mouse apoE differs significantly from human apoE in regulating Aβ metabolism (mouse apoE stimulates Aβ deposition, but human apoE stimulates Aβ clearance), as demonstrated in the current and previous studies (77, 78, 92), drugs that work well in $hAPP_{FAD}$ mice with mouse apoE might not work well in AD patients with human apoE. This might explain at least to some extent the unsatisfactory outcome of many clinical trials targeting Aβ (99). Thus, $hAPP_{FAD}$ mice expressing different forms of human apoE are more reliable models for preclinical studies of drugs targeting Aβ. However, in $hAPP_{FAD}$ mice expressing human apoE3 or apoE4, significant Aβ accumulation usually appears after 12–16 months of age. Thus, $hAPP_{FAD}$/apoE4(Δ272–299)/mEKO mice, which develop significant Aβ accumulation and neuronal and behavioral deficits at 6–8 months of age, represent an alternative mouse model for studying anti-AD drugs targeting both Aβ and apoE4.

Previously, it was reported that neuronal and behavioral deficits were observed in transgenic mice expressing high levels of C-terminal-truncated apoE4 fragments at a young age (6–7 months) (29) or low levels in old age (12–13 months) (59). The data reported here show that low levels of apoE4 fragments elicit marginal neuronal and behavioral deficits in young mice (5–9 months). However, in combination with low levels of Aβ, which alone do not cause deficits (100, 101), apoE4 fragments lead to significant premature death and more pronounced neuronal and behavioral deficits in mice at a young age. Thus, although Aβ is not necessary for apoE4 fragments to be involved in neuropathology, low levels of both cause early-onset neuronal and behavioral deficits in mice. Importantly, mice expressing apoE4 fragments accumulated similar levels of Aβ*56 as hAPP/mEKO mice ($p = 0.05$, Fig. 10*B*), despite overall lower levels of Aβ; however, it is not clear whether this was due to increased formation or decreased clearance of Aβ*56 in the presence of apoE4 fragments. The greater abundance of apoE4 fragments in AD brains than in age-matched controls (28, 29) might facilitate Aβ*56 accumulation, contributing to learning and memory deficits. Thus, in mice, apoE4 fragments alone elicit neuronal and behavioral deficits, and the additional presence of Aβ or Aβ*56, even at low levels of each, accelerates the deficits. ApoE4 fragments may act in the same way to contribute to the pathogenesis and lower the age of onset of AD in humans. Consequently, apoE4 cleavage should also be considered a target for anti-AD drug development (24, 36, 37, 60).

CHAPTER 5

Future Studies

To identify potential novel apoE receptor(s) mediating Aβ clearance. As described in Introduction/Literature Review section, it has been suggested that the lipid-binding domain (aa 244–272) of apoE binds with Aβ peptides (48, 61, 63) to mediate their clearance through the LDL receptor and/or the LDL receptor–related protein (LRP1) pathways (102, 103). ApoE interacts with the LDL receptor and LRP1 through its receptor-binding domain (aa 135–150) in the N-terminus of the molecule (22). However, two paradoxical facts do not support these conclusions. First, the apoE2 isoform has impaired LDL receptor binding due to the presence of the cysteine-158. If clearance of the apoE-Aβ complex is indeed regulated by LDL receptor–mediated uptake of the complex from the extracellular milieu, apoE2 carriers would have highly increased Aβ levels and accelerated accumulation. Since this is clearly not the case in human brain samples, and apoE2 binding to Aβ is generally not impaired, other receptor(s) may exist which mediate the uptake of apoE-Aβ complexes for clearance. Second, as demonstrated in the current study, mouse apoE does not clear Aβ efficiently in the brain, although it does bind well with Aβ, the LDL receptor, and the LRP1. This again suggests the potential existence of an unknown receptor that mediates the clearance of apoE-Aβ complexes. The current study demonstrated that apoE4(Δ272–299) cleared Aβ with ~25% efficiency of the full-length apoE in mouse brains. While impaired Aβ binding of apoE4(Δ272–299) may partially explain the decreased Aβ clearance, possible

interactions in the last 27 amino acids of apoE with an unknown receptor could also explain the phenomenon. That is, potential binding of the C-terminus (aa 272–299) of apoE to an unknown receptor may be a contributing mechanism of Aβ clearance mediated by apoE. Interestingly, the greatest difference in primary sequence between mouse and human apoE resides within this region (aa 272–299), which represents a good starting point in the development of experiments to identify the unknown receptor(s) in future studies.

Although many genome-wide association studies (GWAS) have been conducted to date that consistently confirm the association of apoE4 with AD (2), it is interesting that susceptibility loci for an apoE receptor or a potential apoE-cleaving enzyme (AECE) have not been identified. One possibility for this is that the differences of apoE4 versus apoE3 in their intrinsic properties to bind with the receptor or to be cleaved by the protease are actually determinants for Aβ clearance and apoE proteolysis (not the receptor or AECE), respectively. In this case, the putative receptor or the AECE may not contribute to apoE4-related increase in AD risk. Another possibility is that the contribution of the putative receptor or AECE variations to AD risk would show up only within the same apoE genotype group. In other words, the genetic variations of the putative receptor or AECE might modify the risk of AD under a given apoE genotype (such as apoE3/3 or apoE4/4) but not across different apoE genotypes. Since all GWAS studies only compare apoE4 carriers with non-carriers (apoE3/3) in terms of their AD risk, any contributions of the putative receptor or AECE variations might not be identified or masked by the strong apoE4 effect due to the study design. Thus, it would be very interesting and important to reanalyze the GWAS data by grouping the samples into

apoE3/3 subjects with or without AD and apoE4/4 (may also include apoE4/3) subjects with or without AD to potentially identify AD susceptibility loci that modify AD risk within the same apoE genotype group. Finally, apoE fragment levels may need to reach a critical threshold to exert toxicity and thus, their detrimental properties might not be regulated by AECE levels and/or activity but rather by clearance and/or degradation. In this case, the clearance and/or degradation of apoE4 fragments is the major determinant for the levels of apoE4 fragments and, thus, the genetic variations of the enzyme itself may not be associated with AD risk.

To explore the detailed mechanisms underlying the concerted effects of apoE4 fragments and Aβ. Many of the findings in this study revealed that the single transgenic mice, either expressing apoE4(Δ272–299) or $hAPP_{FAD}$ alone, did not demonstrate significant deficits or impairments at young ages. However, in the presence of the C-terminal-truncated apoE4 fragment, there was evidence of toxicity in young mice even though the levels of Aβ were less than those in apoE null mice. In this study, the observed impairments were attributed to the concerted toxicity induced by both apoE4 fragment and possibly Aβ*56 oligomers. The poor interaction between the apoE4 fragment with Aβ may lead to decreased Aβ clearance as discussed, leading to increased Aβ* formation. However, apoE4 fragments might directly affect Aβ* formation, the formation of other toxic Aβ assembly states, such as dimers or trimers, or their degradation.

In addition, how exactly apoE4 fragments, which are toxic to the mitochondria and the cytoskeleton of neurons, and Aβ oligomers, which may aberrantly bind post-synaptic

receptors to induce calcium dyshomeostasis and LTP impairments (104, 105), cooperate to cause neuronal and cognitive deficits is unknown. Does the accumulation of one protein before the other serve to initiate cellular stress pathways that might further weaken cellular responses to another insult? To test whether one toxic agent functions in first initiating cellular damage, an *in vitro* model such as primary neuronal cultures may be beneficial. Using primary neurons from mice expressing apoE4(Δ272–299), the neurotoxic effect of various amounts of Aβ oligomers can be assessed. The experiment can be reversed so that the apoE4 fragment is variably expressed in the presence of low amounts of Aβ oligomers. Calcium and redox-sensitive dyes can be utilized to measure excitotoxicity and perturbations in mitochondrial function, respectively. Live-cell imaging of labeled mitochondria or other tagged mitochondrial proteins can be assessed for impairments in mitochondrial motility. ApoE4 trafficking through the secretory pathway is impaired in primary neurons (89), and thus, similar strategies can also be pursued.

To explore the importance of apoE4 fragments in cognitive decline in humans. The current study also demonstrated that the onset of neuronal and behavioral impairments was detected at a relatively young age in the presence of both apoE4 fragments and low levels of Aβ. How these findings compare to human cases of preclinical or prodromal AD is unknown. Are there correlations between levels of apoE4 fragment and Aβ in human cerebral spinal fluid or plasma with age or degree of cognitive decline? C-terminal-truncated apoE4 can be detected in plasma and is believed to be derived from the CNS. Levels of apoE4 fragments can also be assessed in cerebral spinal fluid as well.

Ongoing studies that attempt to correlate the extent of apoE4 fragmentation with levels of Aβ and cognition in young and aged human samples will add important insights towards understanding the relative contribution of apoE4 fragments to Aβ-dependent and Aβ-independent neuronal and cognitive deficits in AD.

References

1. Golde, T.E., Schneider, L.S., and Koo, E.H. 2011. Anti-Aβ therapeutics in Alzheimer's disease: the need for a paradigm shift. *Neuron* 69:203–213.

2. Bertram, L., Lill, C.M., and Tanzi, R.E. 2010. The genetics of Alzheimer's disease: back to the future. *Neuron* 68:270–281.

3. Kamenetz, F., Tomita, T., Hsieh, H., Seabrook, G., Borchelt, D., Iwatsubo, T., Sisodia, S., and Malinow, R. 2003. APP processing and synaptic function. *Neuron* 37:925–937.

4. Weyer, S.W., Klevanski, M., Delekate, A., Voikar, V., Aydin, D., Hick, M., Fllippov, M., Drost, N., Schaller, K.L., Saar, M., et al. 2011. APP and APLP2 are essential at PNS and CNS synapses for transmission, spatial learning and LTP. *EMBO J.*:Early online publication.

5. Cirrito, J.R., Yamada, K.A., Finn, M.B., Sloviter, R.S., Bales, K.R., May, P.C., Schoepp, D.D., Paul, S.M., Mennerick, S., and Holtzman, D.M. 2005. Synaptic activity regulates interstitial fluid amyloid-β levels in vivo. *Neuron* 48:913–922.

6. Puzzo, D., Privitera, L., Fa, M., Staniszewski, A., Hashimoto, G., Aziz, F., Sakurai, M., Ribe, E.M., Troy, C.M., Mercken, M., et al. 2011. Endogenous amyloid-β is necessary for hippocampal synaptic plasticity and memory. *Ann. Neurol.* 69:819–830.

7. Hardy, J., and Selkoe, D.J. 2002. The amyloid hypothesis of Alzheimer's disease: progress and problems on the road to therapeutics. *Science* 297:353–356.

8. Verbeek, M.M., Ruiter, D.J., and Waal, R.M.d. 1997. The role of amyloid in the pathogenesis of Alzheimer's disease. *Biol. Chem.* 378:937–950.

9. Wisniewski, T., Ghiso, J., and Frangione, B. 1997. Biology of Aβ amyloid in Alzheimer's disease. *Neurobiol. Dis.* 4:313–328.

10. Podlisny, M.B., Ostaszewski, B.L., Squazzo, S.L., Koo, E.H., Rydell, R.E., Teplow, D.B., and Selkoe, D.J. 1995. Aggregation of secreted amyloid β-protein into sodium dodecyl sulfate-stable oligomers in cell culture. *J. Biol. Chem.* 270:9564–9570.

11. Podlisny, M.B., Walsh, D.M., Amarante, P., Ostaszewski, B.L., Stimson, E.R., Maggio, J.E., Teplow, D.B., and Selkoe, D.J. 1998. Oligomerization of endogenous and synthetic amyloid β-protein at nanomolar levels in cell culture and stabilization of monomer by congo red. *Biochemistry* 37:3602–3611.

12. Mucke, L., Masliah, E., Yu, G.-Q., Mallory, M., Rockenstein, E.M., Tatsuno, G., Hu, K., Kholodenko, D., Johnson-Wood, K., and McConlogue, L. 2000. High-level neuronal expression of $A\beta_{1-42}$ in wild-type human amyloid protein precursor transgenic mice: Synaptotoxicity without plaque formation. *J. Neurosci.* 20:4050–4058.

13. Buttini, M., Yu, G.-Q., Shockley, K., Huang, Y., Jones, B., Masliah, E., Mallory, M., Yeo, T., Longo, F.M., and Mucke, L. 2002. Modulation of Alzheimer-like synaptic and cholinergic deficits in transgenic mice by human apolipoprotein E depends on isoform, aging, and overexpression of amyloid β peptides but not on plaque formation. *J. Neurosci.* 22:10539–10548.

14. Palop, J.J., Jones, B., Kekonius, L., Chin, J., Yu, G.-Q., Raber, J., Masliah, E., and Mucke, L. 2003. Neuronal depletion of calcium-dependent proteins in the dentate

gyrus is tightly linked to Alzheimer's disease-related cognitive deficits. *Proc. Natl. Acad. Sci. USA* 100:9572–9577.

15. Cheng, I.H., Palop, J.J., Esposito, L.A., Bien-Ly, N., Yan, F., and Mucke, L. 2004. Aggressive amyloidosis in mice expressing human amyloid peptides with the Arctic mutation. *Nat. Med.* 10:1190–1192.

16. Roberson, E.D., Scearce-Levie, K., Palop, J.J., Yan, F., Cheng, I.H., Wu, T., Gerstein, H., Yu, G.-Q., and Mucke, L. 2007. Reducing endogenous tau ameliorates amyloid β–induced deficits in an Alzheimer's disease mouse model. *Science* 316:750–754.

17. Lesné, S., Koh, M.T., Kotilinek, L., Kayed, R., Glabe, C.G., Yang, A., Gallagher, M., and Ashe, K.H. 2006. A specific amyloid-beta protein assembly in the brain impairs memory. *Nature* 440:352–357.

18. Lambert, M.P., Barlow, A.K., Chromy, B.A., Edwards, C., Freed, R., Liosatos, M., Morgan, T.E., Rozovsky, I., Trommer, B., Viola, K.L., et al. 1998. Diffusible, nonfibrillar ligands derived from $A\beta_{1-42}$ are potent central nervous system neurotoxins. *Proc. Natl. Acad. Sci. USA* 95:6448–6453.

19. Meilandt, W.J., Cisse, M., Ho, K., Wu, T., Esposito, L.A., Scearce-Levie, K., Cheng, I.H., Yu, G.Q., and Mucke, L. 2009. Neprilysin overexpression inhibits plaque formation but fails to reduce pathogenic Aβ oligomers and associated cognitive deficits in human amyloid precursor protein transgenic mice. *J. Neurosci.* 29:1977–1986.

20. Shankar, G.M., Li, S., Mehta, T.H., Garcia-Munoz, A., Shepardson, N.E., Smith, I., Brett, F.M., Farrell, M.A., Rowan, M.J., Lemere, C.A., et al. 2008. Amyloid-β

protein dimers isolated directly from Alzheimer's brains impair synaptic plasticity and memory. *Nat. Med.* 14:837–842.

21. Harris, J.A., Devidze, N., Verret, L., Ho, K., Halabisky, B., Thwin, M.T., Kim, D., Hamto, P., Lo, I., Yu, G.Q., et al. 2010. Transsynaptic progression of amyloid-β-induced neuronal dysfunction within the entorhinal-hippocampal network. *Neuron* 68:428–441.

22. Mahley, R.W. 1988. Apolipoprotein E: Cholesterol transport protein with expanding role in cell biology. *Science* 240:622–630.

23. Mahley, R.W., and Huang, Y. 1999. Apolipoprotein E: From atherosclerosis to Alzheimer's disease and beyond. *Curr. Opin. Lipidol.* 10:207–217.

24. Huang, Y. 2010. Aβ-independent roles of apolipoprotein E4 in the pathogenesis of Alzheimer's disease. *Trends Mol Med* 16:287–294.

25. Xu, Q., and Huang, Y. 2006. Lipid metabolism in Alzheimer's and Parkinson's disease. *Future Lipidol.* 1:441–453.

26. Weisgraber, K.H. 1994. Apolipoprotein E: Structure–function relationships. *Adv. Protein Chem.* 45:249–302.

27. Morrow, J.A., Hatters, D.M., Lu, B., Höchtl, P., Oberg, K.A., Rupp, B., and Weisgraber, K.H. 2002. Apolipoprotein E4 forms a molten globule: A potential basis for its association with disease. *J. Biol. Chem.* 277:50380–50385.

28. Huang, Y., Liu, X.Q., Wyss-Coray, T., Brecht, W.J., Sanan, D.A., and Mahley, R.W. 2001. Apolipoprotein E fragments present in Alzheimer's disease brains induce neurofibrillary tangle-like intracellular inclusions in neurons. *Proc. Natl. Acad. Sci. USA* 98:8838–8843.

29. Harris, F.M., Brecht, W.J., Xu, Q., Tesseur, I., Kekonius, L., Wyss-Coray, T., Fish, J.D., Masliah, E., Hopkins, P.C., Scearce-Levie, K., et al. 2003. Carboxyl-terminal-truncated apolipoprotein E4 causes Alzheimer's disease-like neurodegeneration and behavioral deficits in transgenic mice. *Proc. Natl. Acad. Sci. USA* 100:10966–10971.

30. Brecht, W.J., Harris, F.M., Chang, S., Tesseur, I., Yu, G.-Q., Xu, Q., Fish, J.D., Wyss-Coray, T., Buttini, M., Mucke, L., et al. 2004. Neuron-specific apolipoprotein E4 proteolysis is associated with increased tau phosphorylation in brains of transgenic mice. *J. Neurosci.* 24:2527–2534.

31. Sakamoto, T., Tanaka, M., Vedhachalam, C., Nickel, M., Nguyen, D., Dhanasekaran, P., Phillips, M.C., Lund-Katz, S., and Saito, H. 2008. Contributions of the Carboxyl-terminal helical segment to the self-association and lipoprotein preferences of human apolipoprotein E3 and E4 isoforms. *Biochemistry* 47:2968–2977.

32. Repa, J.J., Turley, S.D., Lobaccaro, J.-M.A., Medina, J., Li, L., Lustig, K., Shan, B., Heyman, R.A., Dietschy, J.M., and Mangelsdorf, D.J. 2000. Regulation of absorption and ABC1-mediated efflux of cholesterol by RXR heterodimers. *Science* 289:1524–1529.

33. Boyles, J.K., Pitas, R.E., Wilson, E., Mahley, R.W., and Taylor, J.M. 1985. Apolipoprotein E associated with astrocytic glia of the central nervous system and with nonmyelinating glia of the peripheral nervous system. *J. Clin. Invest.* 76:1501–1513.

34. Pitas, R.E., Boyles, J.K., Lee, S.H., Foss, D., and Mahley, R.W. 1987. Astrocytes synthesize apolipoprotein E and metabolize apolipoprotein E-containing lipoproteins. *Biochim. Biophys. Acta* 917:148–161.

35. Sun, Y., Wu, S., Bu, G., Onifade, M.K., Patel, S.N., LaDu, M.J., Fagan, A.M., and Holtzman, D.M. 1998. Glial fibrillary acidic protein–apolipoprotein E (apoE) transgenic mice: Astrocyte-specific expression and differing biological effects of astrocyte-secreted apoE3 and apoE4 lipoproteins. *J. Neurosci.* 18:3261–3272.

36. Huang, Y., Weisgraber, K.H., Mucke, L., and Mahley, R.W. 2004. Apolipoprotein E. Diversity of cellular origins, structural and biophysical properties, and effects in Alzheimer's disease. *J. Mol. Neurosci.* 23:189–204.

37. Mahley, R.W., Weisgraber, K.H., and Huang, Y. 2006. Apolipoprotein E4: A causative factor and therapeutic target in neuropathology, including Alzheimer's disease. *Proc. Natl. Acad. Sci. USA* 103:5644–5651.

38. Nathan, B.P., Bellosta, S., Sanan, D.A., Weisgraber, K.H., Mahley, R.W., and Pitas, R.E. 1994. Differential effects of apolipoproteins E3 and E4 on neuronal growth in vitro. *Science* 264:850–852.

39. Bellosta, S., Nathan, B.P., Orth, M., Dong, L.-M., Mahley, R.W., and Pitas, R.E. 1995. Stable expression and secretion of apolipoproteins E3 and E4 in mouse neuroblastoma cells produces differential effects on neurite outgrowth. *J. Biol. Chem.* 270:27063–27071.

40. Brodbeck, J., Balestra, M.E., Saunders, A.M., Roses, A.D., Mahley, R.W., and Huang, Y. 2008. Rosiglitazone increases dendritic spine density and rescues spine

loss caused by apolipoprotein E4 in primary cortical neurons. *PNAS* 105:1343–1346.

41. Dumanis, S.B., Tesoriero, J.A., Babus, L.W., Nguyen, M.T., Trotter, J.H., Ladu, M.J., Weeber, E.J., Turner, R.S., Xu, B., Rebeck, G.W., et al. 2009. ApoE4 decreases spine density and dendritic complexity in cortical neurons in vivo. *J. Neurosci.* 29:15317–15322.

42. Chen, Y., Lomnitski, L., Michaelson, D.M., and Shohami, E. 1997. Motor and cognitive deficits in apolipoprotein E-deficient mice after closed head injury. *Neuroscience* 80:1255–1262.

43. Slooter, A.J.C., Tang, M.-X., van Duijn, C.M., Stern, Y., Ott, A., Bell, K., Breteler, M.M.B., Van Broeckhoven, C., Tatemichi, T.K., Tycko, B., et al. 1997. Apolipoprotein E ε4 and the risk of dementia with stroke. A population-based investigation. *J. Am. Med. Assoc.* 277:818–821.

44. Poirier, J., Baccichet, A., Dea, D., and Gauthier, S. 1993. Cholesterol synthesis and lipoprotein reuptake during synaptic remodelling in hippocampus in adult rats. *Neuroscience* 55:81–90.

45. Trommer, B.L., Shah, C., Yun, S.H., Gamkrelidze, G., Pasternak, E.S., Ye, G.L., Sotak, M., Sullivan, P.M., Pasternak, J.F., and LaDu, M.J. 2004. ApoE isoform affects LTP in human targeted replacement mice. *Neuroreport* 15:2655–2658.

46. Namba, Y., Tomonaga, M., Kawasaki, H., Otomo, E., and Ikeda, K. 1991. Apolipoprotein E immunoreactivity in cerebral amyloid deposits and neurofibrillary tangles in Alzheimer's disease and kuru plaque amyloid in Creutzfeldt–Jakob disease. *Brain Res.* 541:163–166.

47. Wisniewski, T., and Frangione, B. 1992. Apolipoprotein E: A pathological chaperone protein in patients with cerebral and systemic amyloid. *Neurosci. Lett.* 135:235–238.

48. Strittmatter, W.J., Saunders, A.M., Schmechel, D., Pericak-Vance, M., Enghild, J., Salvesen, G.S., and Roses, A.D. 1993. Apolipoprotein E: High-avidity binding to β-amyloid and increased frequency of type 4 allele in late-onset familial Alzheimer disease. *Proc. Natl. Acad. Sci. USA* 90:1977–1981.

49. Schmechel, D.E., Saunders, A.M., Strittmatter, W.J., Crain, B.J., Hulette, C.M., Joo, S.H., Pericak-Vance, M.A., Goldgaber, D., and Roses, A.D. 1993. Increased amyloid β-peptide deposition in cerebral cortex as a consequence of apolipoprotein E genotype in late-onset Alzheimer disease. *Proc. Natl. Acad. Sci. USA* 90:9649–9653.

50. Corder, E.H., Saunders, A.M., Strittmatter, W.J., Schmechel, D.E., Gaskell, P.C., Small, G.W., Roses, A.D., Haines, J.L., and Pericak-Vance, M.A. 1993. Gene dose of apolipoprotein E type 4 allele and the risk of Alzheimer's disease in late onset families. *Science* 261:921–923.

51. Saunders, A.M., Schmader, K., Breitner, J.C.S., Benson, M.D., Brown, W.T., Goldfarb, L., Goldgaber, D., Manwaring, M.G., Szymanski, M.H., McCown, N., et al. 1993. Apolipoprotein E ε4 allele distributions in late-onset Alzheimer's disease and in other amyloid-forming diseases. *Lancet* 342:710–711.

52. Strittmatter, W.J., and Roses, A.D. 1995. Apolipoprotein E and Alzheimer disease. *Proc. Natl. Acad. Sci. USA* 92:4725–4727.

53. Corder, E.H., Saunders, A.M., Risch, N.J., Strittmatter, W.J., Schmechel, D.E., Gaskell, P.C., Jr., Rimmler, J.B., Locke, P.A., Conneally, P.M., Schmader, K.E., et al. 1994. Protective effect of apolipoprotein E type 2 allele for late onset Alzheimer disease. *Nat. Genet.* 7:180–184.

54. Buttini, M., Orth, M., Bellosta, S., Akeefe, H., Pitas, R.E., Wyss-Coray, T., Mucke, L., and Mahley, R.W. 1999. Expression of human apolipoprotein E3 or E4 in the brains of *Apoe*$^{-/-}$ mice: Isoform-specific effects on neurodegeneration. *J. Neurosci.* 19:4867–4880.

55. Raber, J., Wong, D., Buttini, M., Orth, M., Bellosta, S., Pitas, R.E., Mahley, R.W., and Mucke, L. 1998. Isoform-specific effects of human apolipoprotein E on brain function revealed in *ApoE* knockout mice: Increased susceptibility of females. *Proc. Natl. Acad. Sci. USA* 95:10914–10919.

56. Raber, J., Wong, D., Yu, G.-Q., Buttini, M., Mahley, R.W., Pitas, R.E., and Mucke, L. 2000. Apolipoprotein E and cognitive performance. *Nature* 404:352–354.

57. Hartman, R.E., Wozniak, D.F., Nardi, A., Olney, J.W., Sartorius, L., and Holtzman, D.M. 2001. Behavioral phenotyping of GFAP-apoE3 and -apoE4 transgenic mice: ApoE4 mice show profound working memory impairments in the absence of Alzheimer's-like neuropathology. *Exp. Neurol.* 170:326–344.

58. Bour, A., Grootendorst, J., Vogel, E., Kelche, C., Dodart, J.-C., Bales, K., Moreau, P.-H., Sullivan, P.M., and Mathis, C. 2008. Middle-aged human apoE4 targeted-replacement mice show retention deficits on a wide range of spatial memory tasks. *Behavioral Brain Res.* 193:174–182.

59. Andrews-Zwilling, Y., Bien-Ly, N., Xu, Q., Li, G., Bernardo, A., Yoon, S.Y., Zwilling, D., Yan, T.X., Chen, L., and Huang, Y. 2010. Apolipoprotein E4 causes age- and Tau-dependent impairment of GABAergic interneurons, leading to learning and memory deficits in mice. *J. Neurosci.* 30:13707–13717.

60. Huang, Y. 2006. Molecular and cellular mechanisms of apolipoprotein E4 neurotoxicity and potential therapeutic strategies. *Curr. Opin. Drug Discov. Dev.* 9:627–641.

61. Strittmatter, W.J., Weisgraber, K.H., Huang, D.Y., Dong, L.-M., Salvesen, G.S., Pericak-Vance, M., Schmechel, D., Saunders, A.M., Goldgaber, D., and Roses, A.D. 1993. Binding of human apolipoprotein E to synthetic amyloid β peptide: Isoform-specific effects and implications for late-onset Alzheimer disease. *Proc. Natl. Acad. Sci. USA* 90:8098–8102.

62. Kim, J., Basak, J.M., and Holtzman, D.M. 2009. The role of apolipoprotein E in Alzheimer's disease. *Neuron* 63:287–303.

63. Pillot, T., Goethals, M., Najib, J., Labeur, C., Lins, L., Chambaz, J., Brasseur, R., Vandekerckhove, J., and Rosseneu, M. 1999. β-Amyloid peptide interacts specifically with the carboxy-terminal domain of human apolipoprotein E: Relevance to Alzheimer's disease. *J. Neurochem.* 72:230–237.

64. Wisniewski, T., Castaño, E.M., Golabek, A., Vogel, T., and Frangione, B. 1994. Acceleration of Alzheimer's fibril formation by apolipoprotein E *in vitro*. *Am. J. Pathol.* 145:1030–1035.

65. Sanan, D.A., Weisgraber, K.H., Russell, S.J., Mahley, R.W., Huang, D., Saunders, A., Schmechel, D., Wisniewski, T., Frangione, B., Roses, A.D., et al. 1994.

Apolipoprotein E associates with β amyloid peptide of Alzheimer's disease to form novel monofibrils. Isoform apoE4 associates more efficiently than apoE3. *J. Clin. Invest.* 94:860–869.

66. LaDu, M.J., Pederson, T.M., Frail, D.E., Reardon, C.A., Getz, G.S., and Falduto, M.T. 1995. Purification of apolipoprotein E attenuates isoform-specific binding to β-amyloid. *J. Biol. Chem.* 270:9039–9042.

67. LaDu, M.J., Falduto, M.T., Manelli, A.M., Reardon, C.A., Getz, G.S., and Frail, D.E. 1994. Isoform-specific binding of apolipoprotein E to β-amyloid. *J. Biol. Chem.* 269:23403–23406.

68. Tokuda, T., Calero, M., Matsubara, E., Vidal, R., Kumar, A., Permanne, B., Zlokovic, B., Smith, J.D., Ladu, M.J., Rostagno, A., et al. 2000. Lipidation of apolipoprotein E influences its isoform-specific interaction with Alzheimer's amyloid β peptides. *Biochem. J.* 348:359–365.

69. Bales, K.R., Verina, T., Dodel, R.C., Du, Y., Altstiel, L., Bender, M., Hyslop, P., Johnstone, E.M., Little, S.P., Cummins, D.J., et al. 1997. Lack of apolipoprotein E dramatically reduces amyloid β-peptide deposition. *Nat. Genet.* 17:263–264.

70. Holtzman, D.M., Bales, K.R., Wu, S., Bhat, P., Parsadanian, M., Fagan, A.M., Chang, L.K., Sun, Y., and Paul, S.M. 1999. Expression of human apolipoprotein E reduces amyloid-β deposition in a mouse model of Alzheimer's disease. *J. Clin. Invest.* 103:R15–R21.

71. Irizarry, M.C., Rebeck, G.W., Cheung, B., Bales, K., Paul, S.M., Holtzman, D.M., and Hyman, B.T. 2000. Modulation of Aβ deposition in APP transgenic mice by an apolipoprotein E null background. *Ann. N. Y. Acad. Sci.* 920:171–178.

72. Hirsch-Reinshagen, V., Maia, L.F., Burgess, B.L., Blain, J.-F., Naus, K.E., McIsaac, S.A., Parkinson, P.F., Chan, J.Y., Tansley, G.H., Hayden, M.R., et al. 2005. The absence of ABCA1 decreases soluble apoE levels but does not diminish amyloid deposition in two murine models of Alzheimer disease. *J. Biol. Chem.* 280:43243–43256.

73. Koldamova, R., Staufenbiel, M., and Lefterov, I. 2005. Lack of ABCA1 considerably decreases brain apoE level and increases amyloid deposition in APP23 mice. *J. Biol. Chem.* 280:43224–43235.

74. Wahrle, S.E., Jiang, H., Parsadanian, M., Hartman, R.E., Bales, K.R., Paul, S.M., and Holtzman, D.M. 2005. Deletion of *Abca1* increases Aβ deposition in the PDAPP transgenic mouse model of Alzheimer disease. *J. Biol. Chem.* 280:43236–43242.

75. Holtzman, D.M., Bales, K.R., Tenkova, T., Fagan, A.M., Parsadanian, M., Sartorius, L.J., Mackey, B., Olney, J., McKeel, D., Wozniak, D., et al. 2000. Apolipoprotein E isoform-dependent amyloid deposition and neuritic degeneration in a mouse model of Alzheimer's disease. *Proc. Natl. Acad. Sci. USA* 97:2892–2897.

76. Fagan, A.M., Watson, M., Parsadanian, M., Bales, K.R., Paul, S.M., and Holtzman, D.M. 2002. Human and murine apoE markedly alters Aβ metabolism before and after plaque formation in a mouse model of Alzheimer's disease. *Neurobiol. Dis.* 9:305–318.

77. Fryer, J.D., Simmons, K., Parsadanian, M., Bales, K.R., Paul, S.M., Sullivan, P.M., and Holtzman, D.M. 2005. Human apolipoprotein E4 alters the amyloid-β 40:42

ratio and promotes the formation of cerebral amyloid angiopathy in an amyloid precursor protein transgenic model. *J. Neurosci.* 25:2803–2810.

78. Bales, K.R., Liu, F., Wu, S., Lin, S., Koger, D., DeLong, C., Hansen, J.C., Sullivan, P.M., and Paul, S.M. 2009. Human APOE isoform-dependent effects on brain-amyloid levels in PDAPP transgenic mice. *J. Neurosci.* 29:6771–6779.

79. Trommer, B.L., Shah, C., Yun, S.H., Gamkrelidze, G., Pasternak, E.S., Stine, W.B., Manelli, A., Sullivan, P., Pasternak, J.F., and LaDu, M.J. 2005. ApoE isoform-specific effects on LTP: blockade by oligomeric amyloid-β1-42. *Neurobiol. Dis.* 18:75–82.

80. Wellnitz, S., Friedlein, A., Bonanni, C., Anquez, V., Goepfert, F., Loetscher, H., Adessi, C., and Czech, C. 2005. A 13-kDa carboxyl-terminal fragment of apoE stabilizes Aβ hexamers. *J. Neurochem.* 94:1351–1360.

81. Sadowski, M., Pankiewicz, J., Scholtzova, H., Ripellino, J.A., Li, Y., Schmidt, S.D., Mathews, P.M., Fryer, J.D., Holtzman, D.M., Sigurdsson, E.M., et al. 2004. A synthetic peptide blocking the apolipoprotein E/β-amyloid binding mitigates β-amyloid toxicity and fibril formation *in vitro* and reduces β-amyloid plaques in transgenic mice. *Am. J. Pathol.* 165:937–948.

82. Sadowski, M.J., Pankiewicz, J., Scholtzova, H., Mehta, P.D., Prelli, F., Quartermain, D., and Wisniewski, T. 2006. Blocking the apolipoprotein E/amyloid-β interaction as a potential therapeutic approach for Alzheimer's disease. *Proc. Natl. Acad. Sci. USA* 103:18787–18792.

83. Dodart, J.-C., Marr, R.A., Koistinaho, M., Gregersen, B.M., Malkani, S., Verma, I.M., and Paul, S.M. 2005. Gene delivery of human apolipoprotein E alters brain

Aβ burden in a mouse model of Alzheimer's disease. *Proc. Natl. Acad. Sci. USA* 102:1211–1216.

84. Chang, S., Ma, T.R., Miranda, R.D., Balestra, M.E., Mahley, R.W., and Huang, Y. 2005. Lipid- and receptor-binding regions of apolipoprotein E4 fragments act in concert to cause mitochondrial dysfunction and neurotoxicity. *Proc. Natl. Acad. Sci. USA* 102:18694–18699.

85. Jones, P.B., Adams, K.W., Rozkalne, A., Spires-Jones, T.L., Hshieh, T.T., Hashimoto, T., Armin, C.A.F.v., Mielke, M., Bacskai, B.J., and Hyman, B.T. 2011. Apolipoprotein E: isoform specific differences in tertiary structure and interaction with amyloid-β in human Alzheimer brain. *PLoS One* 6:e14586.

86. Dong, L.-M., Wilson, C., Wardell, M.R., Simmons, T., Mahley, R.W., Weisgraber, K.H., and Agard, D.A. 1994. Human apolipoprotein E. Role of arginine 61 in mediating the lipoprotein preferences of the E3 and E4 isoforms. *J. Biol. Chem.* 269:22358–22365.

87. Dong, L.-M., and Weisgraber, K.H. 1996. Human apolipoprotein E4 domain interaction. Arginine 61 and glutamic acid 255 interact to direct the preference for very low density lipoproteins. *J. Biol. Chem.* 271:19053–19057.

88. Xu, Q., Brecht, W.J., Weisgraber, K.H., Mahley, R.W., and Huang, Y. 2004. Apolipoprotein E4 domain interaction occurs in living neuronal cells as determined by fluorescence resonance energy transfer. *J. Biol. Chem.* 279:25511–25516.

89. Brodbeck, J., McGuire, J., Liu, Z., Meyer-Franke, A., Balestra, M.E., Jeong, D.E., Pleiss, M., McComas, C., Hess, F., Witter, D., et al. 2011. Structure-dependent impairment of intracellular apolipoprotein E4 trafficking and its detrimental effects

are rescued by small-molecule structure correctors. *J. Biol. Chem.* 286:17217-17226.

90. Stine, W.B., Jr, Dahlgren, K.N., Krafft, G.A., and LaDu, M.J. 2003. In vitro characterization of conditions for amyloid-β peptide oligomerization and fibrillogenesis. *J. Biol. Chem.* 278:11612–11622.

91. Li, G., Bien-Ly, N., Andrews-Zwilling, Y., Xu, Q., Bernardo, A., Ring, K., Halabisky, B., Deng, C., Mahley, R.W., and Huang, Y. 2009. GABAergic interneuron dysfunction impairs hippocampal neurogenesis in adult apolipoprotein E4 knockin mice. *Cell Stem Cell* 5:634–645.

92. Irizarry, M.C., Cheung, B.S., Rebeck, G.W., Paul, S.M., Bales, K.R., and Hyman, B.T. 2000. Apolipoprotein E affects the amount, form, and anatomical distribution of amyloid β-peptide deposition in homozygous APP^{V717F} transgenic mice. *Acta Neuropathol.* 100:451–458.

93. Buttini, M., Masliah, E., Yu, G.Q., Palop, J.J., Chang, S., Bernardo, A., Lin, C., Wyss-Coray, T., Huang, Y., and Mucke, L. 2010. Cellular source of apolipoprotein E4 determines neuronal susceptibility to excitotoxic injury in transgenic mice. *Am. J. Pathol.* 177:563–569.

94. Grootendorst, J., Enthoven, L., Dalm, S., Kloet, E.R.d., and Oitzl, M.S. 2004. Increased corticosterone secretion and early-onset of cognitive decline in female apolipoprotein E-knockout mice. *Behav. Brain Res.* 148:167–177.

95. Cheng, I.H., Scearce-Levie, K., Legleiter, J., Palop, J.J., Gerstein, H., Bien-Ly, N., Puoliväli, J., Lesné, S., Ashe, K.H., Muchowski, P.J., et al. 2007. Accelerating

amyloid-beta fibrillization reduces oligomer levels and functional deficits in Alzheimer disease mouse models. *J. Biol. Chem.* 282:23818–23828.

96. Tanaka, M., Vedhachalam, C., Sakamoto, T., Dhanasekaran, P., Phillips, M.C., Lund-Katz, S., and Saito, H. 2006. Effect of carboxyl-terminal truncation on structure and lipid interaction of human apolipoprotein E4. *Biochemistry* 45:4240–4247.

97. Chou, C.-Y., Jen, W.-P., Hsieh, Y.-H., Shiao, M.-S., and Chang, G.-G. 2006. Structural and functional variations in human apolipoprotein E3 and E4. *J. Biol. Chem.* 281:13333–13344.

98. Poirier, J. 2005. Apolipoprotein E, cholesterol transport and synthesis in sporadic Alzheimer's disease. *Neurobiol. Aging* 26:355–361.

99. Zahs, K.R., and Ashe, K.H. 2010. 'Too much good news' - are Alzheimer mouse models trying to tell us how to prevent, not cure, Alzheimer's disease? *Trends Neurosci.* 33:381–389.

100. Chin, J., Palop, J.J., Yu, G.Q., Kojima, N., Masliah, E., and Mucke, L. 2004. Fyn kinase modulates synaptotoxicity, but not aberrant sprouting, in human amyloid precursor protein transgenic mice. *J. Neurosci.* 24:4692–4697.

101. Chin, J., Palop, J.J., Puoliväli, J., Massaro, C., Bien–Ly, N., Gerstein, H., Scearce–Levie, K., Masliah, E., and Mucke, L. 2005. Fyn kinase induces synaptic and cognitive impairments in a transgenic mouse model of Alzheimer's disease. *Neurobiol. Dis.* 25:9694–9703.

102. Kim, J., Castellano, J.M., Jiang, H., Basak, J.M., Parsadanian, M., Pham, V., Paul, S.M., and Holtzman, D.M. 2009. Overexpression of low-density lipoprotein

receptor in the brain markedly inhibits amyloid deposition and increase extracellular Aβ clearance. *Neuron* 64:632–644.

103. Shibata, M., Yamada, S., Kumar, S.R., Calero, M., Bading, J., Frangione, B., Holtzman, D.M., Miller, C.A., Strickland, D.K., Ghiso, J., et al. 2000. Clearance of Alzheimer's amyloid-β_{1-40} peptide from brain by LDL receptor–related protein-1 at the blood-brain barrier. *J. Clin. Invest.* 106:1489–1499.

104. Cisse, M., Halabisky, B., Harris, J., Devidze, N., Dubal, D.B., Sun, B., Orr, A., Lotz, G., Kim, D.H., Hamto, P., et al. 2011. Reversing EphB2 depletion rescues cognitive functions in Alzheimer model. *Nature* 469:47–52.

105. Green, K.N., and LaFerla, F.M. 2008. Linking calcium to Aβ and Alzheimer's disease. *Neuron* 59:190–194.

LIBRARY RELEASE FORM

Publishing Agreement

It is the policy of the University to encourage the distribution of all theses, dissertations, and manuscripts. Copies of all UCSF theses, dissertations, and manuscripts will be routed to the library via the Graduate Division. The library will make all theses, dissertations, and manuscripts accessible to the public and will preserve these to the best of their abilities, in perpetuity.

Please sign the following statement:

I hereby grant permission to the Graduate Division of the University of California, San Francisco to release copies of my thesis, dissertation, or manuscript to the Campus Library to provide access and preservation, in whole or in part, in perpetuity.

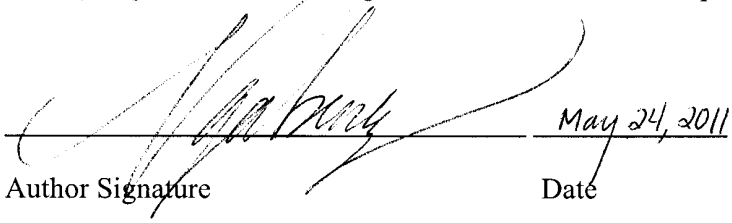

May 24, 2011

Author Signature Date